Journal of Marine Research, 48, 379–412, 1990

Meridional variations of the springtime phytoplankton community in the Sargasso Sea

by D. A. Siegel[1,2], R. Iturriaga[3], R. R. Bidigare[4], R. C. Smith[5], H. Pak[6], T. D. Dickey[7], J. Marra[8], and K. S. Baker[9]

ABSTRACT

Meridional distributions of particle, pigment, optical, chemical and physical *in situ* oceanographic properties, as well as satellite-sensed sea-surface temperature and color imagery, are used to investigate phytoplankton community distributions and their relation to the near-surface water masses of the Sargasso Sea. Measurements were made during April of 1985 along a 1200 km transect on 70W (from 24N to 35N). The seasonal evolution of subtropical Mode water (18° water) is shown to be the primary factor controlling the spatial distribution and evolution of the phytoplankton community in the northern Sargasso Sea (31 to 35N). The springtime near-surface restratification of recently ventilated 18° water initiated a diatom-dominated phytoplankton bloom. As the bloom declined, the phytoplankton community evolved into a diverse assemblage. The consequences of these phytoplankton successions were observed both temporally and as spatial variations along the meridional section. South of the region of 18° water wintertime ventilation (south of 31N), phytoplankton concentrations were considerably less and appeared to be regulated by different processes than the northern region. In particular, influences of subtropical convergence fronts were observed. For the northern Sargasso Sea, the wintertime ventilation of 18° water is shown to be the primary new nutrient flux into the euphotic zone, comprising most of the expected annual new production for this region.

1. Woods Hole Oceanographic Institution, Woods Hole, Massachusetts, 02543, U.S.A.
2. Present address: Department of Geography, 3611 Ellison Hall, University of California at Santa Barbara, Santa Barbara, California, 93106, U.S.A.
3. Department of Biological Sciences, University of Southern California, Los Angeles, California, 90089-0371, U.S.A.
4. Geochemical and Environmental Research Group, Texas A&M University, College Station, Texas, 77843, U.S.A.
5. Marine Bio-Optics Group, Department of Geography, University of California at Santa Barbara, Santa Barbara, California, 93106, U.S.A.
6. College of Oceanography, Oregon State University, Corvallis, Oregon, 97331, U.S.A.
7. Ocean Physics Group, Department of Geological Sciences, University of Southern California, Los Angeles, California, 90089-0740, U.S.A.
8. Lamont Doherty Geological Observatory, Columbia University, Palisades, New York, 10964, U.S.A.
9. Marine Bio-Optics Group, Scripps Institution of Oceanography, University of California at San Diego, La Jolla, California, 92122, U.S.A.

1. Introduction

Distributions of open ocean biological and optical properties and their variability are important for many oceanographic applications, including: the elucidation of primary and secondary production, the examination of carbon fluxes to the deep sea, the modelling of the trophic and successional dynamics of the planktonic ecosystem, and the determination of upper ocean heat budgets. As phytoplankton cells are the primary producers of the sea, knowledge of how the environment influences community structure is primary to the understanding of ocean productivity. Phytoplankton pigment concentrations also control important optical properties, such as the diffuse attenuation coefficient (e.g., Smith and Baker, 1978a,b; Baker and Smith, 1982; Siegel and Dickey, 1987a; Morel, 1988), making knowledge of their distribution and variability important to optical oceanography.

Meridional distributions of bio-optical properties (defined here as those biological parameters which influence light attenuation) and their relationships to the physical environment can provide information concerning probable controlling mechanisms. Mesoscale water mass variations, mixed layer turbulence, and upper layer restratification processes all can affect nutrient availability and particle residence times within the euphotic zone. These physical processes should have significant effects on the structure of the phytoplankton community and hence, the observed bio-optical properties.

Bio-optical properties may be self-regulating in that the phytoplankton assemblage can respond to and reflect variations in the local optical environment. Processes by which this bio-optical self-regulation can occur include photoadaptation of cellular pigment concentration (Eppley *et al.*, 1973; Cullen, 1982; SooHoo *et al.*, 1986; Pak *et al.*, 1988), chromatic adaptation of specific phytoplankton species to the amount and quality of the *in situ* irradiance (Glover *et al.*, 1986, Bidigare *et al.*, 1989a; 1990) and the differential growth of phytoplankton species (Platt *et al.*, 1983; Glover *et al.*, 1985, 1986, 1988; Iturriaga and Marra, 1988), as well as the seasonal succession of algal groups (Hulburt, 1964; Guillard and Kilham, 1977). Grazing processes may also modify the open ocean phytoplankton assemblage (e.g., Roman *et al.*, 1986; Iturriaga and Mitchell, 1986; Huntley *et al.*, 1987; Michaels and Silver, 1988).

Our goal is to examine qualitatively distributional data taken along a meridional transect across the Sargasso Sea and to suggest the influences that the physical and optical environments had on the observed phytoplankton assemblage. In making these interpretations, it is assumed that the observed property variations had been produced locally, rather than having been advected from another region along the transect. The validity of this assumption may be examined by comparing advective time scales with expected time scales for typical biological processes. For example, a meridional length scale of 200 km (~2° latitude) and a mean meridional current of 5 cm s^{-1} results in an advective time scale of roughly 1.5 months. If the controlling processes have time scales of a month or less, the observed variations can be assumed to be locally produced. Many of the processes considered important for pelagic ecological dynamics and

distributions of bio-optical parameters have time scales of a month or less (e.g., Haury *et al.*, 1978; Dickey, 1988). Indeed, satellite color imagery reported here indicates that the time scale for the spring phytoplankton bloom is about 12 days. Thus, the bio-optical distributions to be presented are likely to be the result of local forcings and should be unaffected by advection for the meridional length (and time) scales considered.

Here, observations of meridional trends in physical and bio-optical oceanographic parameters from the western Sargasso Sea made during the spring of 1985 are presented. The specific goals of this study are (1) to investigate the large-scale (200 to 1200 km) spatial variations of springtime phytoplankton abundances and their relationship to the physical and optical environs of the Sargasso Sea, (2) to assess possible mechanisms affecting the abundance and composition of the phytoplankton assemblage and (3) to identify the role of phytoplankton populations in the absorption and scattering of light in the upper layers. Before the distributions of parameters are presented, a climatological context of the observations will be discussed. The reader familiar with the oceanography of the Sargasso Sea may wish to skip past this section.

2. Characteristics of the Sargasso Sea

The Sargasso Sea is commonly defined as the subtropical gyre region of the western North Atlantic Ocean bordered by the Gulf Stream to the north and west, by the North Equatorial Current to the south and by regions of weak recirculation flow to the east. One important feature of the Sargasso Sea is the 18° water mass (Worthington, 1959; Schroeder *et al.*, 1959). The thermohaline properties of the 18° water mass are remarkably stable (over interannual time scales) which are thought to be maintained primarily by intense air-sea heat and freshwater exchanges (Warren, 1972; Talley and Raymer, 1982; Jenkins, 1982). The 18° water mass ventilates to the sea surface during the late winter months generally north of 31N (Ebbesmeyer and Lindstrom, 1986). For the northern Sargasso Sea, wintertime cooling creates convectively-driven mixed layers which are often rather deep (>250 m). During the early spring, the near-surface waters begin to restratify, essentially capping the 18° water mass. This restratification process, in some sense, proceeds northward roughly following the seasonal heating cycle at each meridional location. Horizontal water mass exchanges do occur between the Sargasso Sea and its outer environs through transport via cold-core rings or by the overflowing of Gulf Stream waters (e.g., Lai and Richardson, 1977; Cornillon *et al.*, 1986). However, the water mass properties of the northern Sargasso Sea are rather uniform because of the closed recirculation flow, strong convective modification of near-surface waters and mixing due to mesoscale eddies.

The seasonal cycle of the 18° water ventilation has important implications for the biological properties of the northern Sargasso Sea. Seasonal variations of primary production, phytoplankton and pigment biomass, nutrient, dissolved oxygen, argon and ^{3}He concentrations and deep-sea sinking material fluxes have been reported for Station

S (32N, 65W) (Menzel and Ryther, 1960, 1961; Hulburt *et al.*, 1960; Jenkins and Goldman, 1985; Deuser, 1986; Jenkins, 1988; Spitzer and Jenkins, 1989). These seasonal property variations are caused, in large part, by short-lived, springtime phytoplankton blooms. The intensity of these blooms appears to be correlated with the intensity of winter storms (Menzel and Ryther, 1961), suggesting that the seasonal ventilation of 18° water (and its vertical transport of new nutrients into the euphotic zone) may control the magnitude of primary production.

In the southern portion of the Sargasso Sea (south of ~32N), the 18° water does not ventilate to the sea surface and the surface waters are primarily of subtropical origin (Worthington, 1976). Optical observations (primarily Secchi disk estimates) indicate that the southern Sargasso Sea is considerably less turbid than the northern region (Riley *et al.*, 1949; Simonot and LeTreut, 1986; Lewis *et al.*, 1988). In addition, mesoscale features associated with the thermohaline fronts of the subtropical convergence zone (from 24 to 30N at 70W) have been shown to influence both physical and biological properties (e.g., Voorhis, 1969; Backus *et al.*, 1969; Katz, 1969; Colton *et al.*, 1975). These thermohaline fronts often have highly convoluted spatial structures with horizontal scales of ~100 km, cross-frontal widths of roughly 10 km and decorrelation time scales of roughly a week (Leetmaa and Voorhis, 1978; Voorhis and Bruce, 1982; R. Weller, personal communication, 1989).

The present observations were taken nearly synoptically along a meridional transect (~70W) through the Sargasso Sea (35 to 24N). The meridional distributions represent a mixture of both time and space variations, in the sense that the observed meridional variability may be caused by the sampling being made at a different portion of a similar seasonal cycle. That is, each location along the meridional transect may have its seasonal plankton cycles "initiated" at a different time. It is likely that this springtime "initiation" of the planktonic ecosystem is tightly coupled to the onset of stratification in the near-surface waters of the northern Sargasso Sea. As benign meteorological conditions progress northward, this "initiation" time for the seasonal cycle of the phytoplankton community should also propagate north. For the southern Sargasso Sea, these wintertime water mass renewal events do not occur. Thus, weak seasonal variations in the planktonic ecosystem would be observed.

3. Sampling and measurement techniques

The data presented here were collected aborad the R/V *Knorr* during April 4–15, 1985 from the sea surface to a nominal depth of 250 m. Seven stations were sampled along this transect (Stations 4 through 10), although not all parameters were sampled at each station and depth. Stations 4 and 10 were each occupied for about 4 days and were located at the northern and southern extrema of the meridional transect. The locations of these stations and the shiptrack are superimposed on a sea-surface temperature (SST) satellite image (Fig. 1). On the return transect, several of the stations were reoccupied. In particular, Station 4 was reoccupied, Station 19, for 5

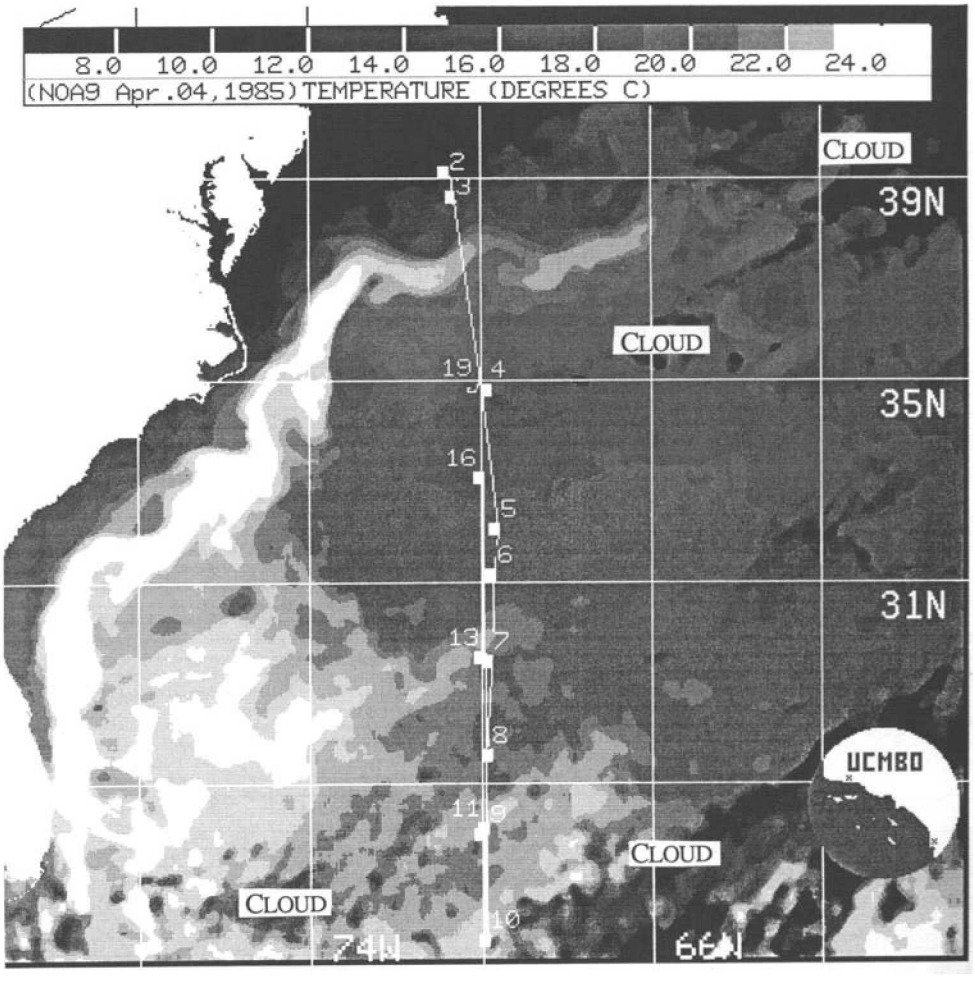

Figure 1. Advanced High Resolution Radiometer (AVHRR) sea surface temperature (SST) image from April 4, 1985 (JD 94). Dark regions correspond to regions of cooler SST. The shiptrack and station locations are also shown.

days, about 2 weeks later (see Smith *et al.* [1989], Marra *et al.* [1990] and Bidigare *et al.* [1990] for details concerning the time series stations).

Vertical profiles of physical and optical parameters were acquired using expendable bathymetric thermographs (XBT), a conductivity-temperature-depth system (CTD), the bio-optical profiling system (BOPS), and an autonomous profiling system, the multi-variable profiler (MVP). From the CTD and BOPS deployments, discrete bottle samples were also taken so that nutrient, particle, pigment, and coccoid cyanobacteria concentrations and particulate absorption spectra could be measured (see Smith *et al.*, 1981, 1984, 1987a, 1989; Bidigare *et al.*, 1987, 1989a; 1990; Pak *et al.*, 1988; Iturriaga

and Marra, 1988 and Marra *et al.*, 1990 for detailed descriptions of the methodologies). In addition, sea-surface temperature and pigment biomass satellite imagery were used to investigate the space/time variability in the area surrounding the shipboard observations.

XBT profiles were made from the surface to a nominal depth of 440 m with a station spacing of 8 minutes of latitude (~15 km). Additional physical oceanographic measurements were made with temperature and conductivity sensors on the CTD and BOPS packages. The BOPS data were used to obtain vertical profiles of the diffuse attenuation coefficient spectrum for downwelling irradiance ($K_d(\lambda)$; see Smith and Baker, 1984). $K_d(\lambda)$ defines the attenuation rate for solar radiation within the upper ocean. Although $K_d(\lambda)$ is by formal definition an apparent optical property (that is, dependent on the geometric distribution of the underwater light field), observations (Baker and Smith, 1980; Siegel and Dickey, 1987a) have shown that $K_d(\lambda)$ is independent of the incident irradiance distribution. Hence, $K_d(\lambda)$ may be considered a quasi-inherent optical property enabling it to be interpreted as a property of a water parcel. Values of the photosynthetic available radiation (PAR) were determined by integrating the observed *in situ* irradiance spectra (Tyler, 1966; Siegel and Dickey, 1987b; Smith *et al.*, 1989). Profiles of the vertical attenuation rate for PAR (K_d(PAR)) and the percentage of incident PAR were also calculated from the irradiance spectra.

The beam attenuation coefficient at 660 nm ($c(660)$) was measured with the BOPS package using a 25 cm SeaTech beam transmissometer (Bartz *et al.*, 1978). The beam attenuation coefficient is defined as the sum of the absorption and scattering coefficients at a specific wavelength. In the open ocean, contributions to $c(660)$ by dissolved materials are generally negligible (Bricaud *et al.*, 1981). Also, observed values of the particulate absorption coefficient at 660 nm were much smaller (<0.004 m^{-1}) than values of the particulate beam attenuation coefficient ($c(660)-c_w(660)$) which ranged from 0.06 to 0.28 m^{-1} (where $c_w(660)$ is the pure water beam attenuation coefficient $\simeq 0.364$ m^{-1}; Bishop, 1986). Thus, variations in the magnitude of $c(660)$ represent changes in particulate scattering which, in turn, reflects the variations in the concentration of scattering particles.

The chloropigment concentration, defined as the sum of the fluorometrically determined chlorophyll *a* and pheopigment concentrations (Smith and Baker, 1978a, 1985), is used as an indicator for the total amount of solar radiation attenuating material. The chloropigment concentration quantifies the total amount of chlorophyll *a*-related pigments in both phytoplankton and detritus. *In situ* optical observations in the open ocean have shown that variations in chloropigment concentrations are well correlated with variations in $K_d(\lambda)$ and K_d(PAR) (e.g., Smith and Baker, 1978a,b; Siegel and Dickey, 1987a,b; Morel, 1988). In a similar manner, the total particle volume (volume of particles with equivalent spherical diameters between 2 and 25 μm per volume of seawater, in units of parts per billion, ppb) is used as an indicator of the total amount of

scattering material that will attenuate a beam of light (e.g., Kitchen *et al.*, 1982; Pak *et al.*, 1988).

The data presented here are primarily in the form of meridional cross-sections. These sections were objectively mapped onto contouring grid points using a least-squares technique (Sampson, 1978). Identical mapping techniques were used for all of the contours shown. The aspect ratio is 57 km in the horizontal direction for every 10 m of depth.

4. Observations

a. The physical environment. An Advanced Very High Resolution Radiometer (AVHRR) SST image for April 4, 1985 (JD 94) is shown in Figure 1; dark regions correspond to regions of cooler SST and probable cloud locations are indicated. Sampling locations (Stations 4 through 19) are also marked on this SST image. Along the shiptrack from 35 to 33N there appeared to be little variation in SST with values of roughly 19C, while near 33N an SST front was discernible. South of this front, the SST distribution exhibited some mesoscale variations. The Gulf Stream is seen as the broad band of warmer water (T > 24C) and it is flowing eastward along 37N.

The cold, circular signature of a Gulf Stream ring occurs near 36N 64W in the AVHRR image (Fig. 1), approximately 700 km ENE of Station 4. This feature was reported as eddy A by the National Oceanic and Atmospheric Administration-National Weather Service (NOAA-NWS) surface feature analysis (Oceanographic Monthly Summary, April 1985). The NOAA-NWS analysis from previous months (Jan.–Mar.) showed this eddy moving toward the west. Another feature (eddy D), near 35N 73W, was first observed on March 3, 1985 (JD 62). However, eddy D moved southward and remained about 300 km from the transect measurements. Thus, it was unlikely that these eddies had directly influenced the oceanographic conditions observed along the meridional transect.

South of 29N, cloudy conditions prevented distinguishing surface SST features from this AVHRR image. However, an AVHRR SST image from April 23, 1985 (JD 113) showed meandering fronts in the region between 26 and 30N. These complicated and convoluted frontal features are part of the subtropical convergence front (SCF; NOAA-NWS analysis from March 29, 1985, JD 88). The NOAA-NWS analysis from April 23, 1985 (JD 113) also showed the SCF crossing 70W three times between 27 and 31N.

During February 1985, the sea-surface temperatures of the western Sargasso Sea were at the seasonal minimum and were on the average 0.5 C cooler than the climatological mean (Oceanographic Monthly Summary, February 1985). Further, the monthly mean 19 C isotherm lay near 30N, along the 70W meridian. An XBT transect made along 65W during February 1985 showed 18° water at the sea surface near 31N (Evans *et al.*, 1985). These data suggest that the winter of 1985 was

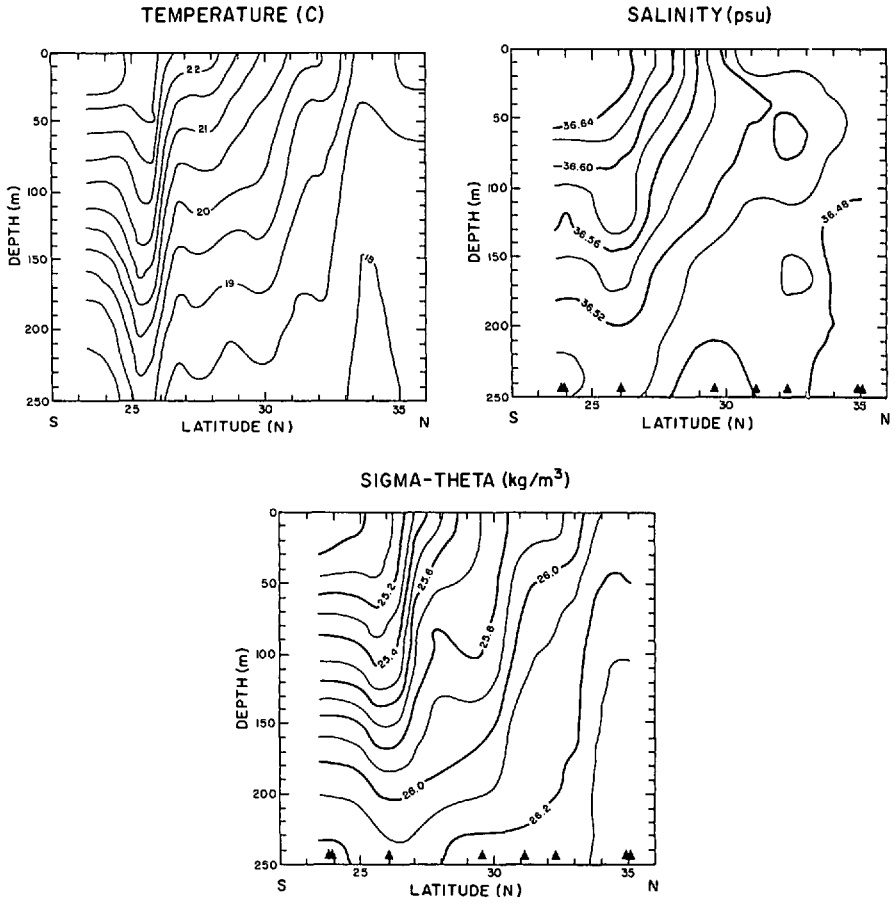

Figure 2. (a) North-south XBT temperature transect. Distance between drops averages ~0.13° in latitude. (b) North-south CTD salinity transect. Location of the CTD stations used are shown by the Δ's on the lower axis. (c) North-south CTD potential density (σ_θ) transect.

relatively intense and that the ventilation of 18° water had occurred throughout a large portion of the northern Sargasso Sea (north of ~31N).

The subsurface temperature field measured with the XBT system is shown in Figure 2a. The dominant features in this distribution were the strong meridional trends in temperature and stratification both of which increased toward the south. In the northernmost region (33–36N), the upper ocean was comprised of weakly stratified 18° water beneath a thin (<50 m) and weakly stratified, near-surface layer. Southward, the 18° water lay progressively deeper within the water column. The steeply descending isotherms between 31 and 33N suggest that subsurface waters may have ventilated to the sea surface in this region. Between 24 and 27N, a large depression in the isotherm displacements (~50 m) was found. This subsurface temperature front was similar in location, isotherm displacement, and horizontal gradient to the subtropical

convergence fronts observed by Voorhis and his collaborators (Voorhis, 1969; Voorhis and Bruce, 1982).

The distribution of salinity (measured with the CTD system) is shown in Figure 2b. Salinity values increased toward the south similar to the meridional temperature trends. However, because of the opposite effects of temperature and salinity upon density, the horizontal salinity gradient reduced the thermally produced, horizontal density gradient (Voorhis and Bruce, 1982). The salinity distribution within the 18° water mass was nearly uniform with a value just greater than 36.48 psu, consistent with the value of 36.50 psu associated with the 18° water mass (Worthington, 1959, 1976). The highest observed salinity values were found within the surface waters at the southern-most station (24N), consistent with the meridional trend of the climatological net freshwater exchange and the subtropical origin of these waters (Worthington, 1976; Schmitt *et al.*, 1989). The subtropical convergence front observed in the XBT section may also be discerned in the salinity section, however the magnitude of the isohaline vertical displacements was not as large. This difference was likely to have been caused by the larger station separations for the CTD deployments compared with the XBT drops.

The meridional trend in stratification was apparent in the potential density distribution (σ_θ; Fig. 2c). Isopycnals within the 18° water were nearly vertical and broadly separated, whereas the tightly spaced isopycnals south of the SCF indicated a higher degree of stratification. The observed value of ~26.3 for the 18° water mass was similar to the climatological mean value of 26.4 (Talley and Raymer, 1982). The SCF was observed with a vertical isopycnal displacement of ~50 m. The density front at the SCF extended throughout the sampled water column (>250 m) and is consistent with the suggestion that the near-surface flow at the SCF is driven by deeper mesoscale eddies (e.g., Voorhis and Bruce, 1982). Throughout the transect, the direction of the horizontal density gradients suggest an eastward flow (relative to 250 m) consistent with the recirculation of the Gulf Stream system (Worthington, 1976).

Meridional variations of SST and mixed layer depth (MLD) obtained from the XBT data are shown in Figure 3. In general, the SST increased toward the south. However, several energetic (~2 C), small horizontal scale (<50 km) SST features were observed, particularly in the vicinity of the SCF (26–27N).

The MLD decreased from roughly 50 m at 34N to ~15 m just north of the SCF (at 26N). The MLD above the 18° water mass may be overestimated because of the weak stratification of the water column. At the SCF, the MLD increased by over 50 m, to a maximum depth of 85 m. South of the SCF, the MLD decreased to about 25 m. The depression of the MLD and isopycnal surfaces at the SCF (Fig. 2c) suggests that the SCF may have been formed from a convergence of mixed layers. Considering the large density front at the SCF, it appeared that this front may have been formed by the convergence of southern subtropical near-surface waters.

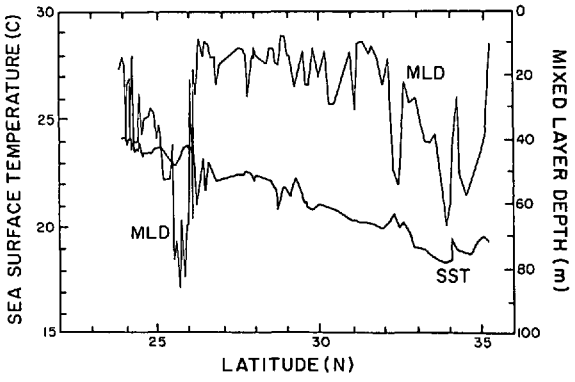

Figure 3. North-south variations of XBT sea surface temperature (SST) (the left axis) and XBT mixed layer depth (MLD) (the right axis). SST is defined here as the mean XBT temperature measured within the upper 5 m. The MLD is defined as that depth where the temperature is less than the SST by 0.1 C.

b. The nutrient fields. Distributions of nitrate and silicate concentrations are shown in Figures 4a and 4b, respectively. Both distributions exhibit elevated concentrations within the 18° water mass suggesting that this water mass may be a source of new nutrients in the northern Sargasso Sea. Significant nitrate concentrations were observed only within the near-surface 18° water mass and below 180 m south of that region (following roughly the 19 C isotherm). Considering that nitrate concentrations are nonconservative, the present value of 1.2–1.3 μM N for the 18° water is not inconsistent with the values of 2 to 3 μM N observed at Station S (Menzel and Ryther, 1960) and values between 1.5 to 2.0 μM N (for the 26.2 σ_θ isopycnal; Kawase and

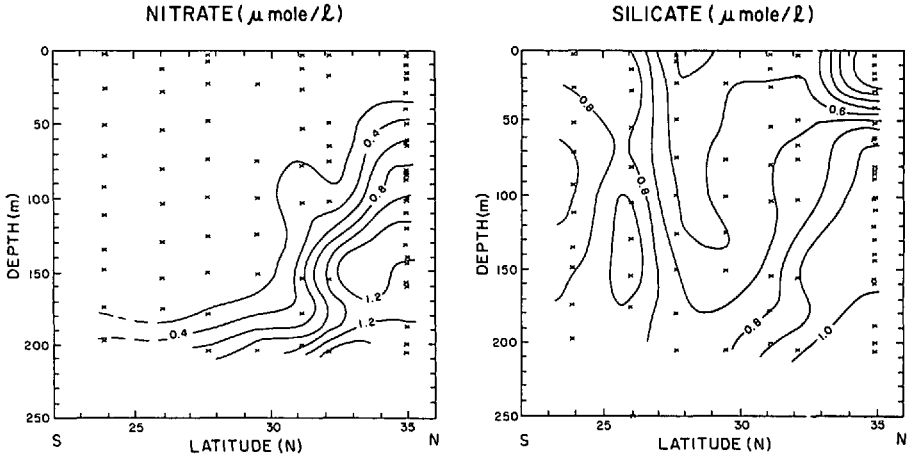

Figure 4. (a) North-south transect of the nitrate concentration (μM N $\equiv$ μmole N l^{-1}). The location of the bottle samples used in the construction of the transect are shown as x's. (b) North-south transect of the silicate concentration (μM Si).

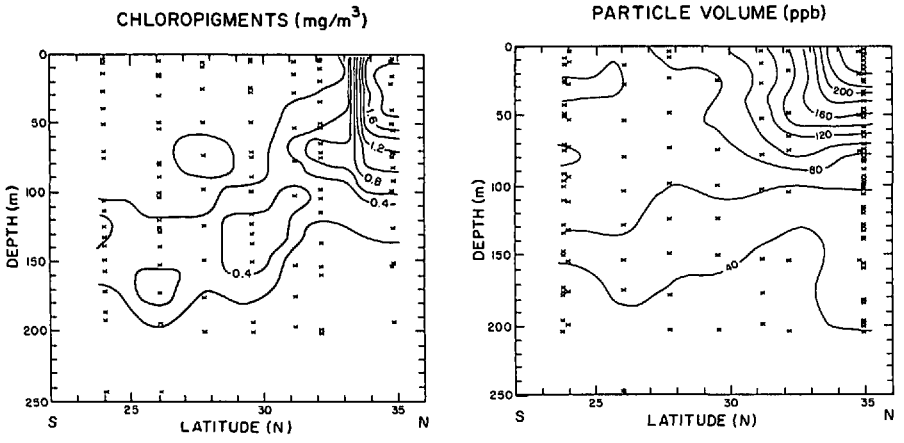

Figure 5. (a) North-south transect of the chloropigment concentration, which is defined as the sum of the fluorometrically determined chlorophyll *a* and pheopigment concentrations (mg m^{-3}). (b) North-south transect of the total particle volume concentration. The volume of particles per volume of sea water is expressed in units of parts per billion (ppb). Total particle volumes are calculated as the sum of all particle volumes with equivalent spherical diameters of 2 to 25 μm.

Sarmiento, 1985, their Fig. 7b). Above the 18° water mass, nitrate concentrations were undetectable because of biological uptake. South of the 18° water mass, the nitracline (defined here as the region between the 0.2 and 0.4 μM N nitrate isopleths) was roughly coincident with the $\sigma_\theta = 26.0$ isopycnal surface and lay at about 180 m southward of 30N. The meridional transect of the nitracline is also shown in Figure 10. Unfortunately, the detailed structure of the nitrate distribution at the SCF cannot be ascertained.

The silicate concentration distribution was roughly the same as the nitrate distribution, however there were several important differences. The lowest observed silicate concentrations (<0.2 μM Si) were found above the 18° water (above 40 m). These extreme low silicate concentrations were likely to be caused by the uptake of this nutrient by diatoms during the phytoplankton bloom observed at Station 4. The silicate concentration within the subsurface 18° water mass was ~1.0 μM Si, which compares well with literature values of 0.5–1.0 μM Si (Kawase and Sarmiento, 1985). In the vicinity of the subtropical convergence front, elevated silicate concentrations were observed throughout the water column and were roughly the same as those observed for the southern (subtropical) mixed layer waters. This supports the notion that the SCF may have been formed by the subduction of subtropical near-surface waters.

c. Chloropigment and total particle distributions. The depth-latitude distribution of the fluorometrically determined chloropigment concentration is shown in Figure 5a. High chloropigment concentrations (>1.8 mg m^{-3}) were observed in the upper 50 m

above the 18° water, consistent with the observed phytoplankton bloom. The magnitude of the presently observed bloom was considerably larger than those observed at Station S by Menzel and Ryther (1960), however their observations were about 200 km south of the present site. A meridional transect of primary production measurements made during the spring of 1959 showed significantly lower production at Station S relative to several northern stations (Ryther and Menzel, 1960).

South of the bloom region, a subsurface chloropigment maximum extended from ~35 m at 32N to a depth of approximately 140 m at 29N. South of 29N, less chloropigment variability was found. Between 32 and 28N, the chloropigment maximum followed the nitracline. However south of the SCF, this relationship was not observed as the nitracline was about 30 m deeper than the chloropigment maximum. Also, in the vicinity of the SCF, downward advection appeared to play some role in the local distribution of the chloropigment concentration. The meridional distribution of the depth of the maximum chloropigment concentration is shown in Figure 10.

The meridional distribution of the total particle volume concentration is shown in Figure 5b. The total particle volume distribution appeared to be similar to the chloropigment distribution (Fig. 5a) where the highest particle volumes were observed within the bloom region (>250 ppb). In contrast with the chloropigment distribution, comparatively high total particle volumes were observed in the upper 80 m between 32 and 30N. There, an indication of a subsurface particle maximum was observed, which lay roughly 50 m above the chloropigment maximum. South of this region, a subsurface particle maximum was not observed. The lack of a correspondence between the subsurface chloropigment maximum and the total particle volume distribution suggests that the chloropigment maximum results from changes in the cellular pigment concentrations, rather than changes in phytoplankton particle volume concentration (e.g., Kiefer *et al.*, 1976; Pak *et al.*, 1988; Fig. 11). However, this interpretation may be incorrect as the resistive-pulse particle counter did not sample particles smaller than ~2 μm nor does it discriminate between phytoplankton and detrital particles (Section 5d; see also Iturriaga and Siegel, 1989).

d. Satellite chlorophyll distributions. Near-surface chlorophyll distributions determined from Coastal Zone Color Scanner (CZCS) images provide an overview of the spatial and temporal phytoplankton pigment variability for the northern Sargasso Sea. Eighteen CZCS images of the study area for the time period between March 13, 1985 (JD 72) through April 28, 1985 (JD 118) were processed using standard CZCS algorithms (Gordon and Clark, 1981). Values of the near-surface chloropigment concentration determined during Station 4 (0.6–0.7 mg m^{-3}) and from a contemporaneous CZCS image (April 5, JD 95; 0.5–0.6 mg m^{-3}) were consistent within the expected 40% tolerance (Smith *et al.*, 1987b).

A CZCS image from March 30 (JD 89; not shown) exhibited relatively high pigment concentrations (0.3–0.6 mg m^{-3}) over a relatively broad area (from 33 to 37N and 68 to 74W). Lower chlorophyll values were observed between 31 and 33N and 70

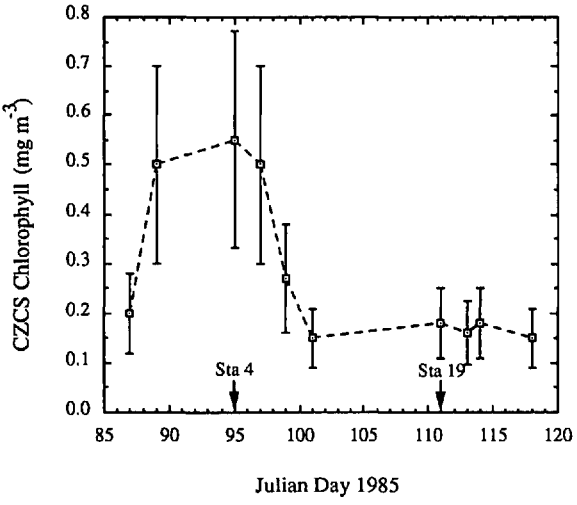

Figure 6. Temporal variations of the mean CZCS near-surface chlorophyll concentrations for the northern Sargasso Sea (generally from 34 to 37N and 75 to 65W). The averaging region varies because of the poor quality of some images (i.e., clouds, improper coverage, etc.). The times of the Station 4 and 19 casts used in Figure 9 are also shown. The error bars represent the 40% error (of the observed) expected in the retrieval of chlorophyll from the CZCS image for this region (Smith *et al.*, 1987b).

and 74W. A CZCS image from March 28 (JD 87; sampled one week prior to the Station 4 observations) showed considerably lower chloropigment concentrations in the vicinity of Station 4 (<0.2 mg m^{-3}; Fig. 6) indicating that a phytoplankton bloom had commenced sometime between JD 87 and 89.

The sequence of available CZCS images allows the temporal evolution of the large spatial scale, near-surface pigment distribution to be addressed. The temporal variations of the mean CZCS chlorophyll concentrations for the northern Sargasso Sea are shown in Figure 6. The bloom observed using the CZCS imagery lasted about 12 days, based upon the CZCS chlorophyll concentrations being greater than 0.5 mg m^{-3}. Thus, the Station 4 observations were made during the bloom while Station 19 observations were made considerably after the near-surface manifestations of the bloom had declined. The location and intensity of the remotely sensed bloom is consistent with the *in situ* chloropigment distribution (Fig. 5a).

It should be noted that the CZCS sensor samples depth-weighted averages of the near-surface chlorophyll distribution (typically the upper 25% of the euphotic zone; Smith *et al.*, 1987b). Subsurface pigment maxima, such as the one found in Figure 5a, will not be sampled with the CZCS satellite sensor. This will act to complicate the interpretation of the bloom's decline.

e. In situ optical property distributions. Distributions of optical properties should reflect (at least to first order) the variations of the amount and type of particulate

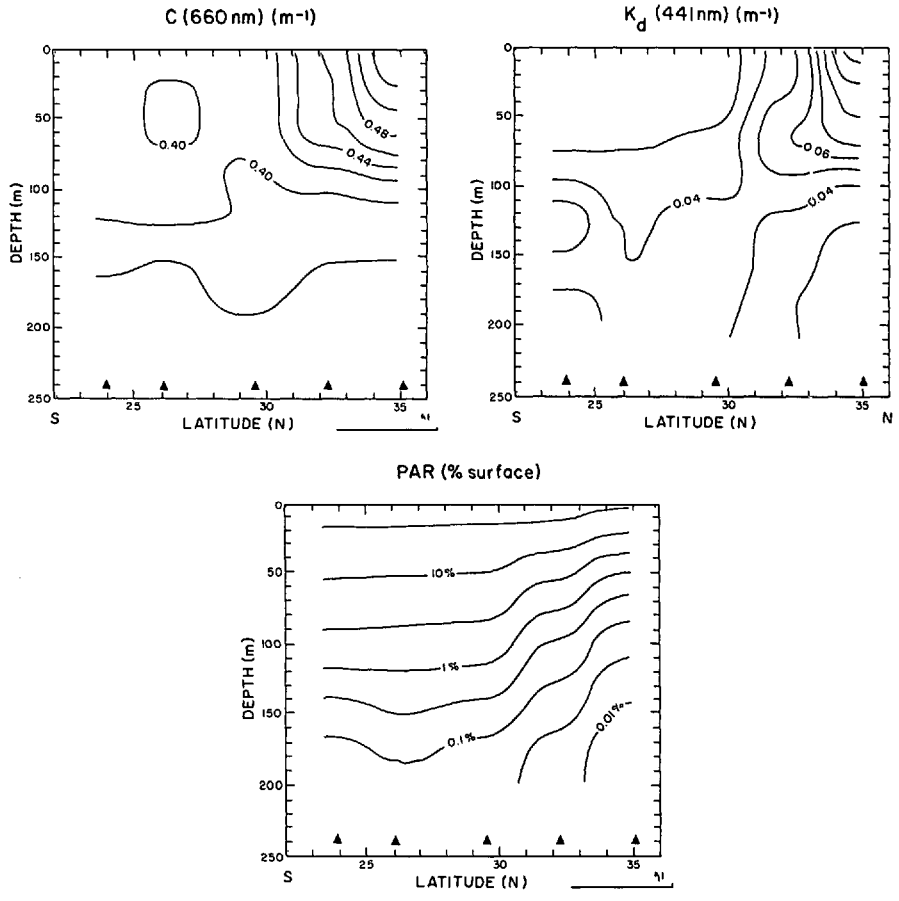

Figure 7. (a) Distribution of the beam attenuation coefficient at 660 nm ($c(660)$). The Δ's represent the location of the BOPS casts used to construct the map. Units are m^{-1}. (b) Distribution of the diffuse attenuation coefficient at 441 nm ($K_d(441)$). Units are m^{-1}. (c) Isopleths of percentage of incident photosynthetic available radiation (%PAR).

material. As first order proxies of the total amount of pigment and particle biomass, optical property distributions should reflect the distributions of the chloropigment and total particle volume concentrations.

As expected, the distributions of the beam attenuation coefficient at 660 nm ($c(660)$; Fig. 7a) and the total particle volume (Fig. 5b) were well correlated ($r = 0.94$; $p < 0.05$), even though the measurement of total particle volume did not include particles smaller than about 2 μm. Elevated values of $c(660)$ were found north of 32N. South of 30N, few significant $c(660)$ variations were observed. Below about 150 m, the magnitude of the $c(660)$ decreased to values less than 0.38 m^{-1} throughout the transect.

The distribution of the diffuse attenuation coefficient at 441 nm ($K_d(441)$; Fig. 7b)

was well correlated ($r = 0.91$; $p < 0.05$) with the chloropigment distribution (Fig. 5a) as expected (e.g., Smith and Baker, 1978b; Siegel and Dickey, 1987a; Morel, 1988). In particular, a subsurface $K_d(441)$ maximum was coincident with the chloropigment maximum. Values of $K_d(441)$ were greater (>0.1 m^{-1}) near the surface at the northern-most station. Elsewhere, magnitudes of $K_d(441)$ were much lower, approaching values found for the clearest ocean waters ($K_w(441) \cong 0.022\ m^{-1}$; Smith and Baker, 1981).

Isopleths of percent photosynthetic available radiation (%PAR) (Fig. 7c) showed deeper penetration of incident PAR in the southern region (south of 30N) compared with the northern Sargasso Sea. This general trend of increasing water clarity toward the south is consistent with climatological trends (Riley *et al.*, 1949; Simonot and LeTreut, 1986; Lewis *et al.*, 1988). The meridional trend for the depth of 1% PAR isopleth, the euphotic zone depth ($Z_{1\%}$), is also shown in Figure 10. The euphotic zone deepened from ~52 m at 35N to about 120 m at 24N.

The depth to which chloropigment concentrations can be remotely sensed using the CZCS satellite sensor (e.g., Smith *et al.*, 1987b) varied from 13 m at Station 4 to 30 m at Station 10. Therefore, the subsurface chloropigment maximum, shown in Figure 5a, would not have been sensed by the CZCS. Further, the interpretation of the bloom's decline based upon the CZCS imagery may be biased by the sampling of only the upper 13 to 30 m of the water column.

f. Indices of the phytoplankton community structure. We use the distributions of five phytoplankton pigments (chlorophyll *a*, fucoxanthin, chlorophyll *b*, 19′-hexanoyloxy-fucoxanthin [hereafter hex-fucoxanthin], and zeaxanthin) as chemotaxonomic source markers for addressing the distributions of phytoplankton biomass (chlorophyll *a*; Fig. 8a), diatoms (fucoxanthin; Fig. 8b), "green" algae (eukaryotic chlorophytes and prasinophytes and prokaryotic prochlorophytes; chlorophyll *b*; Fig. 8c), prymnesiophytes (hex-fucoxanthin; Fig. 8d), and cyanobacteria and prochlorophytes (zeaxanthin; Fig. 8e) (e.g., Jeffrey, 1974, 1976; Lorenzen, 1981; Gieskes and Kraay, 1983a,b; 1986; Guillard *et al.*, 1985; Bidigare *et al.*, 1987; 1990; Smith *et al.*, 1987a; Chisholm *et al.*, 1988). Similarly, distributions of the abundances of coccoid cyanobacteria (Fig. 8f) and 2, 5, and 15 μm spherical diameter particles (Figs. 8g, 8h, and 8i, respectively) are used to describe abundances of several different aspects of the phytoplankton assemblage. Together with the pigment markers, the particle abundance distributions can be used to evaluate the composition of the phytoplankton community.

The chlorophyll *a* concentration distribution (Fig. 8a), which reflects primarily concentrations of living phytoplankton, is similar to the chloropigment distribution (Fig. 5a) as expected. Higher values were observed within the bloom region of Station 4 (>800 ng l^{-1}) and concentrations decreased rapidly with depth. A subsurface chlorophyll *a* maximum was found at 32N at a depth of 70 m which continued southward at depths of 120–150 m. South of 30N, near-surface values of chlorophyll *a*

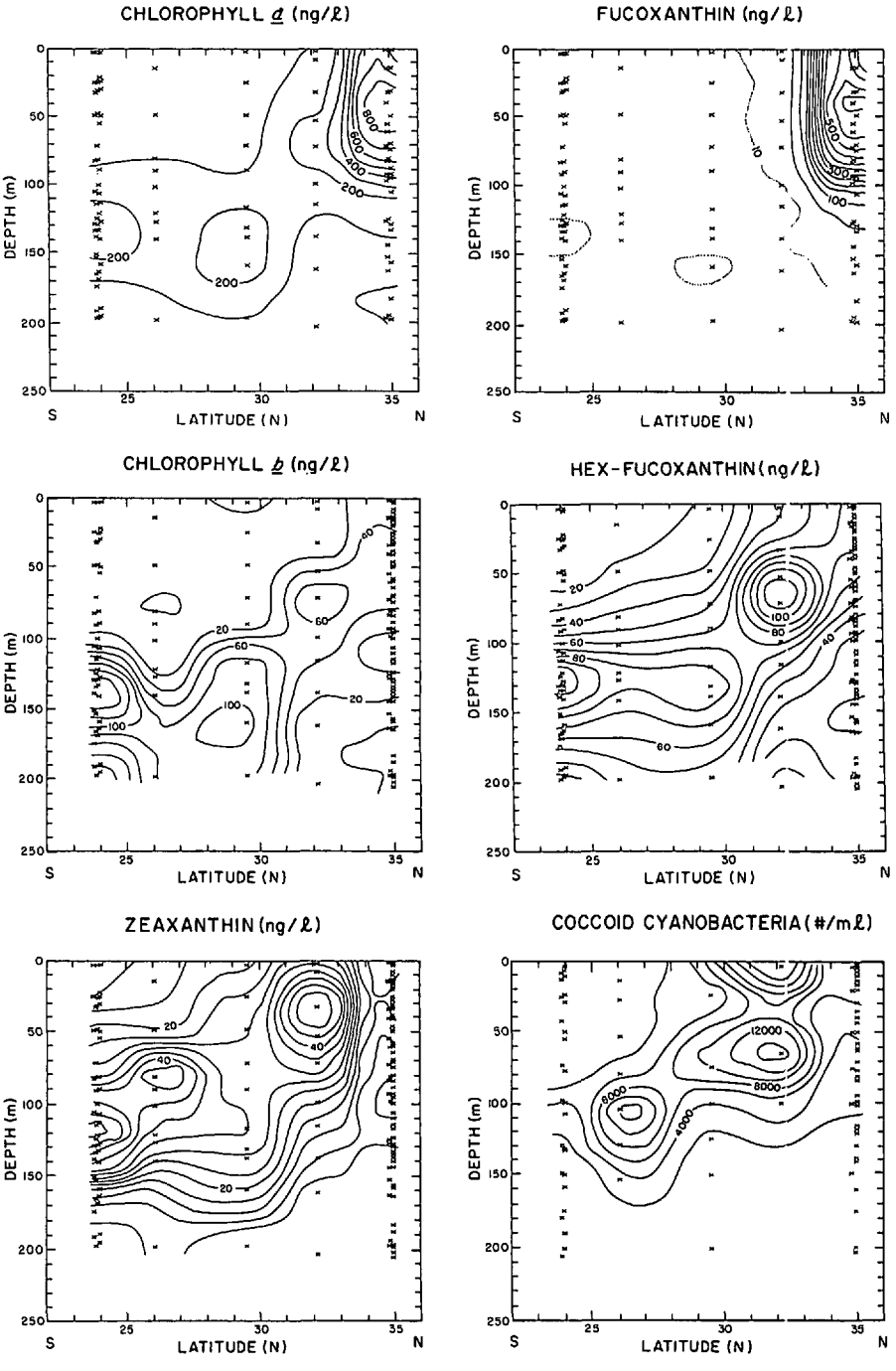
CHLOROPHYLL a (ng/ℓ)
FUCOXANTHIN (ng/ℓ)
CHLOROPHYLL b (ng/ℓ)
HEX-FUCOXANTHIN (ng/ℓ)
ZEAXANTHIN (ng/ℓ)
COCCOID CYANOBACTERIA (#/mℓ)
DEPTH (m)
LATITUDE (N)
S
N
0
50
100
150
200
250
25
30
35
200
400
600
800
10
300
100
20
60
40
80
12000
8000
4000

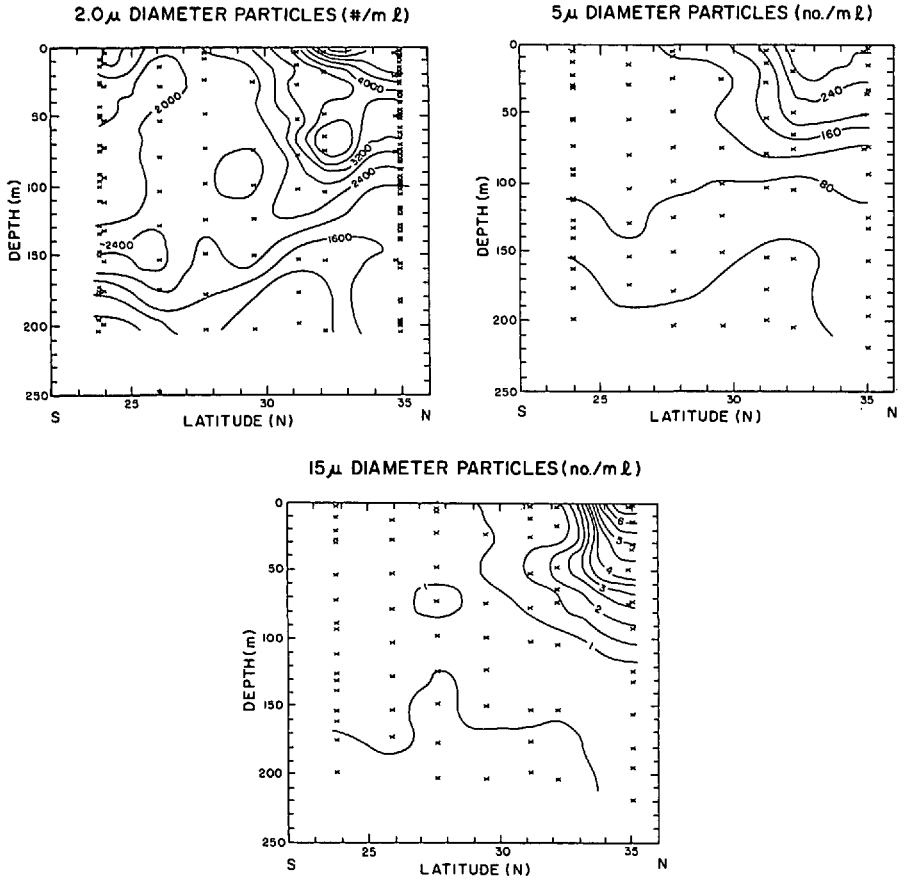

Figure 8. Distributions of the HPLC-determined pigment concentration (ng l^{-1}) and particle abundances (# ml^{-1}): (a) chlorophyll *a*, (b) fucoxanthin, (c) chlorophyll *b*, (d) hex-fucoxanthin, and (e) zeaxanthin, (f) coccoid cyanobacteria abundances (cells per ml), (g) 2 μm diameter particles (# particles with $1.97 < D < 2.21$ μm ml^{-1}), (h) 5 μm diameter particles (# particles with $4.96 < D < 5.57$ μm ml^{-1}) and (i) 15 μm diameter particles (# particles with $14.0 < D < 15.8$ μm ml^{-1}). Locations of the bottle samples are indicated with the x's.

were much less (<100 ng l^{-1}). A comparison of the depths of the chlorophyll *a* maximum with isopleths of %PAR (Fig. 7c) indicates that north of 30N, the chlorophyll *a* maximum tracked the 1% PAR depth (Fig. 10). South of 30N, the chlorophyll *a* maximum lay relatively deeper within the water column (near the 0.3% PAR depth). Between 32 and 28N, the chlorophyll *a* maximum was also observed to follow the nitracline (Fig. 10) suggesting that the depth of the chlorophyll *a* maximum for this region was regulated, at least in part, by the nutrient distribution. South of 29N, the chlorophyll *a* maximum was 30 to 40 m above the depth of the nitracline.

The distribution of fucoxanthin, a pigment source marker for diatom abundances, is shown in Figure 8b. The highest concentrations of fucoxanthin were found within the

phytoplankton bloom at Station 4 with peak values of greater than 600 ng l^{-1}. A comparison of fucoxanthin to chlorophyll *a* ratios (ca. 0.8:1; w:w; Fig. 9a) indicates that diatoms comprised most (~80%) of the chlorophyll *a* phytoplankton biomass at Station 4 (Abaychi and Riley, 1979). Microscopic enumeration of phytoplankton also indicates that diatoms (primarily of the genera *Rhizosolenia* and *Chaetoceros*) were the dominant autotroph at this site (F. Reid, 1987; personal communication). Elsewhere, nearly undetectable fucoxanthin concentrations were observed.

The distribution of chlorophyll *b* (a source marker for eukaryotic and prokaryotic "green" algae; Fig. 8c) was significantly different from the distributions of chloropigment, chlorophyll *a* or fucoxanthin (Figs. 5a, 8a, and 8b, respectively). In particular, the highest chlorophyll *b* concentrations were found within a subsurface maximum south of the bloom site. North of ~30°N, the depth of this subsurface chlorophyll *b* maximum was coincident with the depths of the nitracline and the chloropigment maxima (Fig. 10). South of 30N, the chlorophyll *b* maximum lay slightly deeper than the chloropigment maximum. The highest concentrations of chlorophyll *b* were observed (>140 ng l^{-1}) within the chlorophyll *a* maximum at 24N. There, the weight ratio of chlorophyll *b* to chlorophyll *a* reached an observed maximum value of ~0.7 indicating that "green" algae comprised a large portion of the southern Sargasso Sea phytoplankton community. For the diatom bloom site, "green" algae were not an important component of the bloom community as this ratio was ~0.05.

The distribution of hex-fucoxanthin (a source marker for prymnesiophytes, including coccolithophores) is shown in Figure 8d. This pigment's distribution was qualitatively similar to the chlorophyll *b* distribution, however its subsurface maximum was displaced upward by about 20 to 30 m (near the 5% PAR depth, Fig. 7c). This suggests that algal groups were layered according to light depths along the meridional transect. The highest hex-fucoxanthin concentrations were found just south of the bloom site (south of 33N). At Station 10 (24N), a subsurface maximum of hex-fucoxanthin concentration was observed, just below the 1% PAR depth and roughly coincident with the chlorophyll *a* maximum.

Zeaxanthin concentrations (Fig. 8e) are often used to indicate abundances of coccoid cyanobacteria (e.g., Gieskes and Kraay, 1983a; Guillard *et al.*, 1985) although deep-living, chlorophyll *b*-containing prochlorophytes also possess zeaxanthin (Chisholm *et al.*, 1988). The highest observed zeaxanthin concentrations occurred within a relatively shallow, subsurface maximum that lay at a depth of 30 m at 32N (the 10% PAR depth) and at 120 m at 24N (the 1% PAR depth). This subsurface maximum was shallow relative to the other subsurface pigment maxima and may be related to the relatively shallow subsurface maxima observed for coccoid cyanobacteria abundances (e.g., Murphy and Haugen, 1985; Iturriaga and Marra, 1988) and/or to the use of zeaxanthin as a photoprotective pigment (Gieskes and Kraay, 1986; Bidigare *et al.*, 1989b).

Epifluorescence microscopy counts of coccoid cyanobacteria (Fig. 8f) showed their highest abundances (>20,000 cells ml^{-1}) in the region north of the SCF and south of the bloom site (between 26N and 33N). The depth of the subsurface cyanobacteria maximum lay near the 2% PAR depth throughout the transect and was slightly shallower than the zeaxanthin maximum (Fig. 8e). Between 26N and 24N, the maximum abundance decreased from over 12,000 cells ml^{-1} to approximately 4,000 cells ml^{-1}, suggesting that the subtropical convergence front may act as a floristic boundary (Iturriaga and Marra, 1988). Previous observations have shown that SCF's act as boundaries for not only phytoplankton abundances, but for many species of zooplankton and fish as well (Hulburt, 1964, 1966; Backus *et al.*, 1969; Colton *et al.*, 1975). Relatively low cyanobacteria abundances were observed at the bloom site (Fig. 8f). South of 32N, cyanobacteria abundances were greater while the total particle volume concentrations (Fig. 5b) were substantially less.

The distributions of coccoid cyanobacteria abundance and zeaxanthin concentration were generally similar (Figs. 8e and 8f). However at 24N (south of the SCF), the correspondence breaks down where relatively low cyanobacteria abundances and high zeaxanthin concentrations were observed. A statistical analysis of the same bottle samples along the transect found no significant correlation between these two measures of the coccoid cyanobacteria abundances ($r = 0.34$; $n = 36$, $p > 0.05$). This result indicates that zeaxanthin may be an inadequate chemotaxonomic source marker for cyanobacteria abundances. It is possible that the high zeaxanthin concentrations measured south of the SCF may reflect prochlorophyte abundances (Chisholm *et al.*, 1988). Also, since the reverse-phase HPLC technique employed was not capable of separating lutein from zeaxanthin, the observed discrepancies may result from the methodologies used. However, recent HPLC/diode array measurements performed on samples collected from the Sargasso Sea (34N 70W) during 1987 indicate that this peak is dominated by zeaxanthin (R. R. Bidigare, unpublished data, 1988).

The distribution of 2 μm diameter particles represents the abundance of picoplankton sized particles (Fig. 8g). The distribution of 2 μm particles was considerably different from the total particle volume distribution (Fig. 5b) where a subsurface maximum was observed throughout much of the meridional transect. Relatively high abundances of 2 μm particles were observed within the bloom. However, these particles made a small contribution to the total particle volume (~17 ppb for the 2 μm particles vs. ~250 ppb for the total particle volume). High abundances were also observed to coincide with the cyanobacteria maximum (near 32N at 60–70m). The subsurface maximum of 2 μm particles extended from 60–70 m at 32N to 140–150 m at 24N. North of 32N, the 2 μm particle maximum was roughly coincident with the depth of the nitracline (Fig. 10) and the cyanobacteria subsurface maximum (Fig. 8f). Between 30 and 28N, the depth of the subsurface maximum for 2 μm particles was consistent with the depth of the hex-fucoxanthin maximum (Fig. 8d) and lay at the 0.3% PAR depth. South of 26N, the depth of the 2 μm particle maximum followed the chlorophyll

b maximum (Fig. 8c). These observations suggest that the 2 μm particle maximum was comprised primarily of coccoid cyanobacteria between 32 and 30N, prymnesiophytes between 30 and 28N, and "green" algae south of 26N.

The meridional distribution of 5 μm particles is shown in Figure 8h. This distribution, which represents the abundance of small nanoplankton sized particles, appeared similar to the distribution of the total particle volume (Fig. 5b). Generally, high abundances of 5 μm particles were observed north of 30N, not just within the bloom region. This was consistent with the relatively high abundances of total particle volumes observed for this region. Similar 5 μm particle abundances were measured in the upper layers of the two northernmost stations (north of 32N), although total particle volumes were higher at the northernmost station. Presumably these differences were caused by a greater contribution from larger sized particles at the bloom site. It also appeared that particles with equivalent diameters of about 5 μm made dominant contributions to the qualitative patterns of the total particle volume (Fig. 5b) and *c*(660) distributions (Fig. 7a).

The distribution of 15 μm particles (Fig. 8i) exhibited its highest abundances within the diatom bloom at the northernmost station. The fact that the total particle volume distribution showed its highest concentrations within the diatom bloom indicates that the bloom was dominated by relatively large ($D > 15$ μm) particles. The major difference between the 5 and 15 μm particle distributions was that high abundances of 5 μm particles were observed at 31 and 32N whereas relatively few of the larger particles were found. In addition, a significant subsurface maximum in the 15 μm particle abundance was observed between 31 and 32N at a depth of about 50 m.

5. Discussion

The distributional data presented here demonstrate that meridional variations of the phytoplankton community (and hence, bio-optical properties) were affected to a large degree by the ambient physical and optical environment. In the following, the response of the phytoplankton assemblage to spatial variations of the physical and optical environs will be addressed in greater detail. Possible mechanisms controlling the spatial structure of the phytoplankton community will be discussed, as well as the contributions that phytoplankton populations make to light attenuation in the Sargasso Sea.

a. 18° water ventilation, diatom blooms, new production and bio-optical properties. It is proposed that the dominant process controlling the meridional distribution of phytoplankton abundances and bio-optical properties in the northern Sargasso Sea (that is, north of 33N) is the blooming of recently ventilated 18° water. Nutrient concentrations are elevated within this water mass relative to typical wintertime near-surface concentrations. These newly upwelled nutrients are rapidly utilized following the springtime formation of near-surface stratification which reduces mixing

rates, enabling phytoplankton populations to be exposed to levels of PAR adequate for sustained photosynthetic production. The bloom community should then be dominated by those algal species, here diatoms, that can rapidly incorporate the elevated nutrient concentrations (e.g., Eppley *et al.*, 1969; Guillard and Kilham, 1977). The increase in pigment and particle concentrations during the phytoplankton bloom then results in increased rates of light attenuation for the upper layers. This conceptual model of the coupling among the processes of physical water mass evolution, phytoplankton blooming (often dominated by diatoms) and decreasing optical clarity is consistent with the historical record of the northern Sargasso Sea (e.g., Riley, 1957; Ryther and Menzel, 1960; Menzel and Ryther, 1960, 1961; Hulburt *et al.*, 1960; Hulburt, 1964).

In the previous discussion, it has been assumed that the existence of the spring phytoplankton bloom was made possible by ventilation of 18° water and its transport of new nutrients into the euphotic zone. Hence, the elevated production due to the new nutrients must be new production (e.g., Eppley and Peterson, 1979). Recent estimates of new production have been made by examining the seasonal variations of dissolved oxygen, ^{3}He and argon concentrations at Station S (Jenkins and Goldman, 1985; Jenkins, 1988; Musgrave *et al.*, 1988; Spitzer and Jenkins, 1989). The magnitude of these new production estimates range from 30 to 50 gC m^{-2} y^{-1} and are about an order of magnitude greater than the new production that can be estimated using the Station S net annual production measurements (Menzel and Ryther, 1961) and typical open ocean recycling efficiencies of 80 to 90% (e.g., Eppley and Peterson, 1979; Harrison, 1980; Jenkins and Goldman, 1985).

A simple estimate of the annual new production produced by 18° water ventilation may be made by assuming that nitrate concentrations are negligible in the upper 150 m during the summer (Menzel and Ryther, 1960) and that nutrient uptake does not occur prior to the spring phytoplankton bloom. The seasonal flux of nitrate into the euphotic zone by convective ventilation processes is estimated to be 0.38 mole N m^{-2} y^{-1} (where a characteristic nitrate concentration of 2.5 μM N for 18° water is used). This corresponds to an annual new production of ~30 gC m^{-2} y^{-1} (using a Redfield ratio of 6.6C:N), consistent with the new production estimates made by Jenkins and his collaborators. This value of new production is likely to be an underestimate as it is assumed that no nutrient uptake occurs prior to the spring bloom (observations at Station S by Dugdale and Goering [1967] showed substantial wintertime nutrient uptake rates). Further, inputs of new nutrients into the euphotic zone from rain or nitrogen fixation are not considered. Thus, the seasonal ventilation of 18° water is likely to be a dominant source of new nutrients for the northern Sargasso Sea.

Our analysis suggests that convectively-driven water mass renewal processes make a greater contribution to the vertical transport of new nutrients to the euphotic zone than do wind-forced turbulent entrainment processes for the northern Sargasso Sea (e.g., Klein and Coste, 1984; Musgrave *et al.*, 1988). This analysis is not meant to minimize the contribution shear-induced mixing and entrainment may make to new production

in the summer and fall seasons (e.g., Lewis *et al.*, 1988; Musgrave *et al.*, 1988). However, these results suggest that local water mass variations can have substantial biological implications and hence, must be taken into account. The circulation patterns which maintain the 18° water of the Sargasso Sea are unusual compared with much of the world ocean, although analogous Mode water regions are found throughout the world ocean (e.g., McCartney, 1982).

b. Post-bloom phytoplankton successions in the northern Sargasso Sea. The seasonal ventilation of 18° water has been shown to be the dominant factor affecting the phytoplankton community structure, bio-optical properties and new production for the northern Sargasso Sea. However, only the coupling between the springtime formation of near-surface stratification and the spring phytoplankton bloom (here, dominated by diatoms) has been discussed. Within the Sargasso Sea, phytoplankton blooms are typically short lived as there is a finite amount of new nutrients available (Riley, 1957; Hulburt, *et al.*, 1960; Hulburt, 1964). The CZCS chlorophyll observations indicate that the bloom described in this study lasted only about 12 days (Fig. 6). Thus, the diatom dominated community will evolve into a community where the dominant algae can grow efficiently at lower ambient nutrient concentrations (e.g., Guillard and Kilham, 1977; Parsons *et al.*, 1984).

The post-bloom succession of the phytoplankton community may be evaluated by comparing phytoplankton parameters measured at Station 4 with those taken at Station 19. These two stations were made 16 days apart at the same site (35N, 70W; see also Fig. 6). Examination of pigment concentrations and microscopic cell counts, revealed that the phytoplankton community had shifted its composition from a diatom-dominated assemblage (Station 4) to a mixed assemblage comprised of "green" algae (including prasinophytes; Bidigare *et al.*, 1987; 1990), prymnesiophytes and coccoid cyanobacteria (Station 19). In particular, near-surface fucoxanthin concentrations at Station 19 (100 ng l^{-1}) were considerably less than those observed at Station 4 (600 ng l^{-1}). However at Station 19, chlorophyll *a* concentrations remained high with peak values greater than 500 ng l^{-1} within a 50 m deep subsurface maximum. This compositional change is better illustrated by comparing the weight ratios of fucoxanthin to chlorophyll *a* for the two stations (Fig. 9a). This ratio indicates that at Station 4, diatoms were the dominant autotroph while at Station 19 they were a relatively minor contributor. Significant temporal differences were also observed in the weight ratios of chlorophyll *b*, hex-fucoxanthin and zeaxanthin to chlorophyll *a* (not shown) indicating that these pigment groups made significantly greater contributions to the Station 19 assemblage than to the one at Station 4 (Bidigare *et al.*, 1990). These data indicate that the diatom-dominated bloom community had succeeded to a mixed assemblage in the time between these two stations.

The particle abundance data may also be used to evaluate the post-bloom phytoplankton successional processes. The abundance of 15 μm sized particles for the Station 4

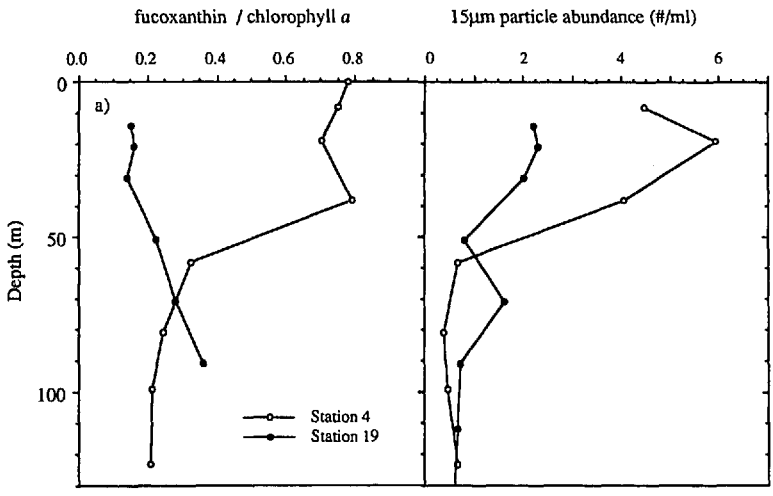

Figure 9. Representative profiles of phytoplankton parameters from Station 4 (open circles) and Station 19 (solid circles). Both stations were sampled at 35N 70W; Station 4 on April 5 (JD 95) and Station 19 on April 21, 1985 (JD 111). (a) Fucoxanthin to chlorophyll *a* weight ratio. (b) Abundance of 15 μm particles (number per ml).

and 19 observations are shown in Figure 9b. These data (and others not shown) indicate that the abundance of relatively large particles (≥10 μm) in the upper 50 m was higher for the diatom bloom community than in the post-bloom assemblage. These large particles were replaced by smaller cells (5 μm and less) as found during the Station 19 observations which may be better able to compete for the low nutrient resources because of their higher relative surface area (e.g., Parsons *et al.*, 1984).

One important question is what happens to the diatom cells after the near-surface bloom has subsided. Although higher abundances of 15 μm particles were observed in the upper 50 m during the bloom (Station 4) than after it (Station 19; Fig. 9b), more of these same particles were found after the bloom between 50 and 90 m. An increase was also observed for this depth range in the fucoxanthin to chlorophyll *a* weight ratios (Fig. 9a). These data suggest that diatoms had accumulated between 50 and 90 m in the time between the two stations.

Many diatom species are capable of increasing their sinking rates in response to a reduction in ambient nutrient concentrations (e.g., Smetacek, 1985; Granata, 1987). This self-regulation of cell buoyancy enables them to sink to regions of higher nutrient concentrations where they may grow more efficiently (e.g., Smetacek, 1985; Goldman, 1988). For Station 19, nitrate concentrations are undetectable above 50 m. Thus, the present observations were consistent with this adaptive strategy. An alternative hypothesis is that the diatoms may simply be growing efficiently at this depth (which is near the 1% PAR depth; Fig. 7c). Several other processes may also have contributed to the removal of diatom cells from the euphotic zone, in particular the rapid sinking of aggregated diatom flocs.

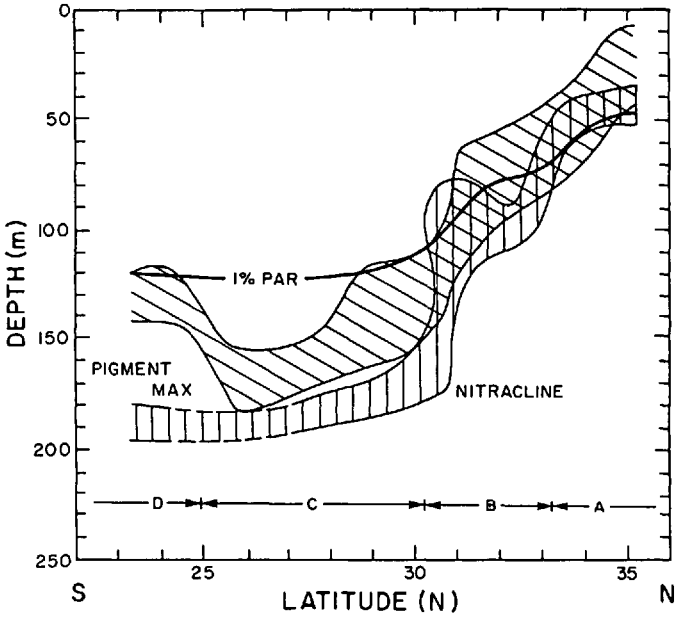

Figure 10. North/south transects of the depths of the fluorometric chloropigment maximum region (chl_{max}), the nitracline (defined as the region between the 0.2 and 0.4 μM N l^{-1} isopleths), and the depth of the euphotic zone (depth of the 1% PAR isopleth [$Z_{1\%}$]; dark solid line). The four specified meridional regions (regions A through D) are discussed in the text.

c. 18° water, nutrients, light, and the chloropigment maximum. We have shown that the effects of the 18° water mass upon the phytoplankton community were most significant where its ventilation to the sea surface had occurred. However, its effects may be observed throughout the entire meridional section. In particular, variations in the depth of the chloropigment maximum were controlled, at least in part, by 18° water mass variations.

To better illustrate this relationship, the meridional transect has been partitioned into four distinct regions (labelled A-D in Figure 10). Each is based upon the spatial structure of the 18° water mass and its relationship to the chloropigment maximum. Within region A (33 to 35N), 18° water was found near the sea surface and a phytoplankton bloom was observed. Region B (between 30 and 33N) was characterized by weak stratification and steeply ascending isotherms (Fig. 2a). During February 1985, 18° water was observed at the sea surface within this region (Evans *et al.*, 19855 and it is thought that a spring bloom had occurred in this region previous to our observations. The inferred phytoplankton community structure from our observations should represent post-bloom conditions. In region C, (30 to 25N), 18° water did not ventilate to the sea surface during the previous winter. However, because of the close proximity of the nitracline to the chloropigment maximum (~25 m), inputs of nutrients from 18° water may still be important. Region D (25 to 24N) is located south of the

SCF. There, the depth of the chloropigment maximum was separated from the nitracline by about 65 m (Fig. 10).

In the southern portion of the transect (south of 30N, regions C and D in Fig. 10), 18° water does not penetrate into the euphotic zone (Fig. 2a). For these regions, the observed chloropigment distribution may be regulated by a variety of processes which may include: photoadaptation of cellular pigment concentrations, chromatic adaptation by algal group, grazing, and the transport of nutrients by physical processes. Regions C and D differ in their respective depths for the chloropigment maximum and the nitracline (Fig. 10). For region C, the nitracline lay ~25 m below the chloropigment maximum. Thus, it is possible that the transport of nutrients into the euphotic zone from the 18° water (possibly episodic in time) may have significant effects upon the dynamics of the chloropigment maximum for this region. These physical transport processes should be of lesser importance south of the SCF (region D), where the nitracline and the chloropigment maximum are separated vertically by ~65 m and other (biologically mediated) processes should be of greater importance (i.e., grazing, photoadaptation, and nutrient recycling).

The region between 30 to 33N (region B) is an important portion of the transect, lying between the region where 18° water has recently ventilated (A) and where it has remained beneath the euphotic zone (C; Fig. 10). During February 1985, 18° water was found near the sea surface within this region and it is likely that the proper conditions for a phytoplankton bloom were present. If a phytoplankton bloom occurred within this region roughly one month prior to these observations, the composition of the phytoplankton assemblage should be similar to that observed at Station 19. The phytoplankton pigment groups sampled in region B and at Station 19 were similar (primarily representing "green" algae, prymnesiophytes and cyanobacteria). Also, the abundances and vertical structure of the total particle volume and the particle size distributions were similar. In addition, the 15 μm particle distribution showed a subsurface maximum just above the nitracline within region B (Figs. 8i and 10) similar to the Station 19 observations (Fig. 9b). These observations all suggest that analogous successional processes had occurred at these two sites and that the difference between regions A and B is manifest in a difference in the initiation time for the planktonic ecosystem. The initiation time is the onset of the spring bloom which follows the creation of near-surface stratification. As relatively benign conditions propagate towards the north, the initiation of spring blooms should also propagate north. Unfortunately, we are not able to test this hypothesis as CZCS coverage was poor for most of February and March.

The boundary between regions B and C represents the southernmost extent (along 70W) where 18° water has ventilated to the sea surface. As described previously, the ventilation of 18° water can comprise a large portion of the annual new production. It seems reasonable that the southern extent of this 18° water ventilation is regulated by the intensity or possibly duration of winter storms. This should be a major cause of

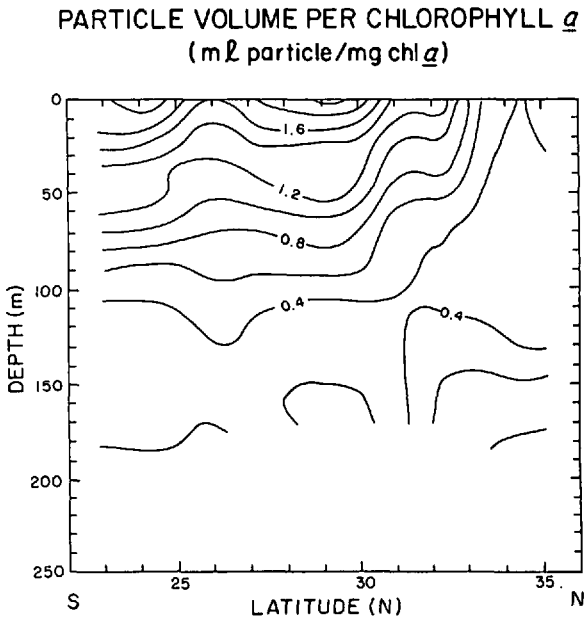

Figure 11. North/south distribution of the ratio of the total particle volume to the concentration of chlorophyll *a* (ml particle per mg chlorophyll *a*). This map was constructed by dividing the gridded fields for the particle volume and chlorophyll *a* concentrations (Sampson, 1978).

interannual variability in the total areal amount of ventilated new production for the Sargasso Sea. In addition, this should be important for observations made in the vicinity of Bermuda (32N, 64W). At that latitude, 18° water mass ventilation may occur depending upon the severity of the previous winter. Similarly, this may lead to large interannual variations in new production, oxygen accumulation and sinking fluxes of particulate materials observed at this site (e.g., Menzel and Ryther, 1961; Jenkins and Goldman, 1985; Deuser, 1986).

d. Photoadaptation processes and phytoplankton community structure. Photoadaptation allows phytoplankton cells to efficiently use light in a variable irradiance environment. The scope of the term photoadaptation is broad and refers to many physiological and biochemical responses, including: photoprotection, chromatic adaptation, changes in photosynthetic pigment concentrations at the cellular level, alterations in chloroplast geometry and pigment packaging.

Elucidation of light-induced responses at the cellular level is problematic because both phytoplankton composition and detrital abundances can vary. For example, the depth-dependent decreases of the total particle volume-to-chlorophyll *a* ratio observed within the southern portion of the transect (Fig. 11) may be attributed to increases in cellular chlorophyll concentrations with depth, or to relatively large numbers of detrital particles in surface waters. The lack of vertical variations of the total particle

volume to chlorophyll *a* ratio at the bloom site (north of 33N) suggests that either the photoadaptation of cellular pigment concentrations is not effective at this site or that this process is effectively masked by detrital particle concentrations. Thus, changes in the concentration ratio of particulates to pigments provide an ambiguous measure of the results of photoadaptation processes.

Phytoplankton pigment distributions measured at Station 4 can be used to examine photoadaptation responses for one algal group, the golden-browns (primarily diatoms and prymnesiophytes). Ratios of the photosynthetically active carotenoids (fucoxanthin and hex-fucoxanthin) to chlorophyll *a* were nearly constant with depth and time (within the upper 40 m of the bloom region), suggesting the absence of a shade-adapted golden-brown algal community at this station (Fig. 9a; Bidigare *et al.*, 1990). This is also consistent with the lack of vertical variations in the total particle volume to chlorophyll *a* ratio (Fig. 11).

Photoprotective processes may also be addressed using the pigment data. At Station 4, the ratio of diadinoxanthin-to-chlorophyll *a* varied as a function of depth and daily irradiance where the highest ratios were found in near-surface waters on sunny days (not shown). Similar responses have been verified in the laboratory using monospecific cultures of chrysophytes, diatoms and dinoflagellates (Mandelli, 1972; Hooks *et al.*, 1988). These results strongly suggest that this photosynthetically inactive carotenoid has a photoprotective function (e.g., Haxo, 1985; Bidigare *et al.*, 1987).

In considering the phytoplankton community along the meridional transect as a whole, evidence for chromatic adaptation as a function of depth and latitude was striking (Figs. 8a–f). At any given station, the major algal groups appeared to be distributed as overlapping layers, with diatoms and cyanobacteria being more abundant closer to the surface and "green" algae and prymnesiophytes more abundant with depth. As the depth of the euphotic zone increased from ~50 m at the northernmost station to 120 m at the southernmost, the depths of the chloropigment and chlorophyll *a* maxima increased, as did the depth intervals between these major algal groups (Figs. 8a–f and 10). Similar algal distributions have been reported in the tropical Atlantic Ocean (Gieskes and Kraay, 1986), in the northwestern Atlantic Ocean (Murphy and Haugen, 1985), and the summertime Sargasso Sea (Glover *et al.*, 1988).

It appeared that the spectral distribution of downwelling irradiance controlled several aspects of the observed algal distributions (e.g., Glover *et al.*, 1986; Bidigare *et al.*, 1990). That is, those algal groups containing photosynthetic pigments which efficiently absorb light in the green (fucoxanthin and phycoerythrin; 500–540 nm) were found most abundant closer to the surface where adequate green light is found to drive photosynthesis (Figs. 8b and f). "Green" algae, which possess the blue-green absorbing pigment chlorophyll *b*, were abundant deeper in the water column (Fig. 8c). The apparent success of the prymnesiophytes is unclear because their pigment composition is generally similar to that of diatoms which were generally restricted to shallow depths. Perhaps their small size in combination with their unique suite of chlorophylls

and carotenoids (hexfucoxanthin and chlorophyll c_3) allowed them to photosynthesize efficiently at intermediate depths.

Thus, it is likely that both chromatic adaptation and photoprotective processes affected the pigment structure of the phytoplankton community along the meridional transect. Other photoadaptation processes, such as alterations of cellular pigment concentrations, may also be important. However, its inference is obscured by the presence of unknown concentrations of detrital materials. In addition, the presence of significant nutrient concentrations at depth (Fig. 4a) will have an influence on the subsurface pigment maxima (see Section 5c).

e. Phytoplankton community structure and optical properties. Variations of the diffuse attenuation coefficient ($K_d(441)$) and the beam attenuation coefficient ($c(660)$) reflect primarily variations in the absorption and scattering properties, respectively. High correspondences were observed between $K_d(441)$ and the chloropigment concentration (Figs. 7b and 5a) and between $c(660)$ and the total particle volume (Figs. 7a and 5b) indicating that variations of these optical properties were well correlated with the respective distributions of the integrated indices of pigment and particle biomass. However, one of our primary objectives is to examine how the composition of the phytoplankton community affects the optical properties of the Sargasso Sea. Obviously, the attenuation of light in the sea is influenced by both phytoplankton and detrital materials. Unfortunately, the presence of unknown concentrations of detrital materials makes the interpretation of the results of the direct statistical comparison between the observed optical properties and phytoplankton distributions ambiguous. Thus, the contributions of the phytoplankton assemblage to $K_d(441)$ and $c(660)$ should be evaluated only in a qualitative sense.

The contributions of the phytoplankton community to $K_d(441)$ may be analyzed by comparing the $K_d(441)$ distribution (Fig. 7b) to those representing aspects of the phytoplankton community structure (Figs. 8a–i). At the northernmost location (Station 4), large ($>10\ \mu$m) diatoms were responsible for the high values of $K_d(441)$ (Figs. 8b, 8i and 9). South of the diatom bloom, elevated values of the diffuse attenuation occurred primarily within a subsurface maximum coincident with the chloropigment maximum (Figs. 5a, 7b and 10). Comparison with the observed particle and pigment distributions showed that the $K_d(441)$ maximum was comprised primarily of relatively small ($2\ \mu$m) particles (Fig. 8g), which consisted of cyanobacteria (Fig. 8f) in region B, prymnesiophytes (Fig. 8d) in region C, and in region D, "green" algae (Fig. 8c). Elsewhere, values of $K_d(441)$ approached values observed for the clearest natural waters ($\sim 0.022\ m^{-1}$; Smith and Baker, 1981). Thus, the phytoplankton population made significant, identifiable contributions to the attenuation of solar radiation within the regions where the pigment concentrations were elevated.

The contributions of particulate materials to the scattering of light can be evaluated by comparing the distribution of the beam attenuation coefficient at 660 nm ($c(660)$;

Fig. 7a) with the observed distributions of the particle size abundances (Figs. 8g–i). As discussed previously, within the diatom bloom the dominant particle sizes were comparatively large ($D > 10$ μm) and their effects upon increases in $c(660)$ were clearly observed. With the exception of the region of previous 18° water ventilation (region B in Fig. 10), values of $c(660)$ were generally low and approached values representing the clearest natural waters (~0.36 m^{-1}; Bishop, 1986). Within region B (Fig. 10), a mixed assemblage of predominantly 5 μm size phytoplankton cells was observed (Figs. 8c–h). There, values of $c(660)$ were elevated above values found just to the south (Fig. 7a) suggesting that the post-bloom phytoplankton community maintained high scattering properties from the initial bloom of large diatoms. Elsewhere, particulate materials made relatively small contributions to $c(660)$.

6. Summary and conclusions

Distributions of *in situ* oceanographic parameters and satellite sea-surface temperature and color imagery have been used to investigate the structure of the springtime phytoplankton community and its relation to upper ocean water mass evolution of the Sargasso Sea. Measurements were made during the spring of 1985 on a 1200 km meridional transect (from 24N to 35N along 70W). The near-surface restratification of recently ventilated 18° water controlled the evolution of the phytoplankton community in the northern Sargasso Sea (31 to 35N) by initiating a phytoplankton bloom dominated by relatively large diatoms. As the diatom bloom declined, the phytoplankton community evolved into a more diverse assemblage, comprised of smaller-sized organisms. These successional processes were observed both temporally and as distributional variations along the meridional transect. Also, the ventilation of 18° water was shown to be the primary upwelling nutrient flux for the annual new production of the northern Sargasso Sea. South of the region of 18° water wintertime ventilation (south of ~31N), oligotrophic conditions were observed. The phytoplankton community for this region was likely to be regulated by different processes than the northern Sargasso Sea. Among the possible processes were chromatic adaptation of the phytoplankton populations, nutrient availability and grazing. Influences of a subtropical convergence front upon the phytoplankton distributions were also observed.

The present work demonstrates some of the roles that phytoplankton succession plays in the evolution of the phytoplankton assemblage and the bio-optical properties in the Sargasso Sea. The proper characterization of the springtime phytoplankton dynamics required that the bloom and post-bloom communities be addressed as separate entities. The detailed phytoplankton pigment and particle size abundance data provided a rich and consistent picture of phytoplankton community variability for the Sargasso Sea. It is hoped that these tools (along with detailed physical oceanographic determinations) will be used extensively in future biological and optical oceanographic experiments.

Acknowledgments. Discussions with Mark Brzezinski, Joan Cleveland, Werner Deuser, Joel Goldman, Tim Granata, Al Hermann, Dale Kiefer, Anthony Michaels and Bob Weller have been helpful. Janet Dodds drafted the computer generated contour plots and Xueyun Zhang assisted with the processing of the CZCS imagery. We have been supported by the Oceanic Biology and Ocean Optics programs of the Office of Naval Research under the following contracts: N00014-87-K-0084 (TDD, DAS), N00014-84-K-0363 (RI), N00014-85-C-0113 (RRB), N00014-84-C-0382 (RCS, KSB), N00014-81-K-0383 (HP), and N00014-84-C-0132-IIA (JM). Additional support for DAS has been provided by the Woods Hole Oceanographic Institution. This is Biowatt contribution number 42 and Woods Hole Oceanographic Institution contribution number 7224.

REFERENCES

Abaychi, J. K. and J. P. Riley. 1979. The determination of phytoplankton pigments by high-performance liquid chromatography. Analytica Chimica Acta, *107,* 1–11.

Backus, R. H., J. E. Craddock, R. L. Haedrich and D. L. Shores. 1969. Mesopelagic fishes and thermal fronts in the western Sargasso Sea. Mar. Biol., *3,* 87–106.

Baker, K. S. and R. C. Smith. 1980. Quasi-inherent characteristics of the diffuse attenuation coefficient for irradiance. Proc. Soc. Photo-Optical Instr. Eng., *208,* Ocean Optics VI, 60–63.

—— 1982. Bio-optical classification and model of natural waters, II. Limnol. Oceanogr., *27,* 500–509.

Bartz, R., H. Pak and J. R. V. Zaneveld. 1978. A transmissometer for profiling and moored observations in water. Proc. Soc. Photo-Optical Instr. Eng., *160,* Ocean Optics V, 102–108.

Bidigare, R. R., J. Marra, T. D. Dickey, R. Iturriaga, H. Pak and R. C. Smith. 1990. Evidence for phytoplankton succession and chromatic adaptation in the Sargasso Sea during springtime 1985. Mar. Ecology Prog. Ser., *60,* 113–122.

Bidigare, R. R., J. H. Morrow and D. A. Kiefer. 1989a. Derivative analysis of spectral absorption by phytoplankton pigments in the western Sargasso Sea. J. Mar. Res., *47,* 323–341.

Bidigare, R. R., O. Schofield, B. B. Prézelin. 1989b. Influence of zeaxanthin on quantum yield of photosynthesis of Synechoccoccus clone WH7803 (DC2). Mar. Ecology Prog. Ser., *56,* 177–188.

Bidigare, R. R., R. C. Smith, K. S. Baker and J. Marra. 1987. Oceanic production estimates from measurements of spectral irradiance and pigment concentrations. Global Biogeochem. Cycles, *1,* 171–186.

Bishop, J. K. B. 1986. The correction and suspended particulate matter calibration of Sea-Tech transmissometer data. Deep-Sea Res., *33,* 121–134.

Bricaud, A., A. Morel and L. Prieur. 1981. Absorption of dissolved organic matter of the sea (yellow substance) in the UV and visible domains. Limnol. Oceanog., *26,* 43–53.

Chisholm, S. W., R. J. Olson, E. R. Zettler, R. Goericke, J. B. Waterbury and N. A. Welschmeyer. 1988. A novel free-living prochlorophyte abundant in the oceanic euphotic zone. Nature, *334,* 340–343.

Colton, Jr., J. B. D. E. Smith and J. W. Jossi. 1975. Further observations on a thermal front in the Sargasso Sea. Deep-Sea Res., *22,* 433–439.

Cornillon, P., D. Evans and W. Large. 1986. Warm outbreaks of the Gulf Stream into the Sargasso Sea. J. Geophys. Res., *91,* 6583–6596.

Cullen, J. J. 1982. The deep chlorophyll maximum: comparing vertical profiles of chlorophyll *a.* Can. Bull. Fish. Aquatic Sci., *39,* 791–803.

Deuser, W. G. 1986. Seasonal and interannual variations in deep-water particle fluxes in the Sargasso Sea and their relation to surface hydrography. Deep-Sea Res., *33,* 225–246.

Dickey, T. D. 1988. Recent advances and future directions in multi-disciplinary *in situ* oceanographic measurement systems, *in* Towards a Theory on Biological-Physical Interactions, B. Rothschild, ed., Kluwer Academic Publishers, NY, 555–598.

Dugdale, R. C. and J. J. Goering. 1967. Uptake of new and regenerated forms of nitrogen in primary productivity. Limnol. Oceanogr., *12,* 196–206.

Ebbesmeyer, C. C. and E. J. Lindstrom. 1986. Structure of 18°C water observed during the POLYMODE local dynamics experiment. J. Phys. Oceanogr., *16,* 443–453.

Eppley, R. W. and B. J. Peterson. 1979. Particulate organic matter flux and planktonic new production in the deep ocean. Nature, *282,* 677–680.

Eppley, R. W., E. H. Renger, E. L. Venrick and M. M. Mullin. 1973. A study of plankton dynamics and nutrient cycling in the central gyre of the North Pacific Ocean. Limnol. Oceanogr., *18,* 534–551.

Eppley, R. W., J. N. Rogers and J. J. McCarthy. 1969. Half-saturation constants for uptake of nitrate and ammonium by marine phytoplankton. Limnol. Oceanogr., *14,* 912–920.

Evans, D., E. Boehm and P. Cornillon. 1985. Observations of the subtropical convergence front at 70W. FASINEX Bulletin, *6,* Sept. 1985, (unpublished manuscript).

Gieskes, W. W. and G. W. Kraay. 1983a. Unknown chlorophyll *a* derivatives in the North Sea and the tropical Atlantic Ocean revealed by HPLC analysis. Limnol. Oceanogr., *28,* 757–766.

—— 1983b. Dominance of Cryptophyceae during the phytoplankton spring bloom in the central North Sea detected by HPLC analysis of pigments. Mar. Biol., *75,* 179–185.

—— 1986. Floristic and physiological differences between the shallow and deep nanophytoplankton community in the euphotic zone of the open tropical Atlantic revealed by HPLC analysis of pigments. Mar. Biol., *91,* 567–576.

Glover, H. E., M. D. Keller and R. R. L. Guillard, 1986. Light quality and oceanic ultraphytoplankters. Nature, *319,* 142–143.

Glover, H. E., B. B. Prézelin, L. Campbell and M. Wyman. 1988. Pico- and ultraplankton Sargasso Sea communities: variability and comparative distributions of *Synechococcus* spp. and algae. Mar. Ecology Prog. Ser., *49,* 127–139.

Glover, H. E., A. E. Smith and L. Shapiro. 1985. Diurnal variations in photosynthetic rates: comparisons of ultraplankton with a larger phytoplankton size fraction. J. Plank. Res., *7,* 519–535.

Goldman, J. C. 1988. Spatial and temporal discontinuities of biological processes in pelagic surface waters, *in* Towards a Theory on Biological-Physical Interactions, B. Rothschild, ed., Kluwer Academic Publishers, NY, 273–296.

Gordon, H. R. and D. K. Clark. 1981. Clear water radiances for atmospheric correction of coastal zone color scanner imagery. Appl. Optics, *20,* 4175–4180.

Granata, T. C. 1987. Measurements of phytoplankton sinking and growth under varied light intensities and mixing regimes. University of California at Berkeley, PhD dissertation, Berkeley, CA, 175 pp.

Guillard, R. R. L. and P. Kilham. 1977. The ecology of marine planktonic diatoms, *in* The Biology of Diatoms, D. Werner, ed., 372–469, Blackwell Sci. Publ., Oxford, U.K.

Guillard, R. R. L., L. S. Murphy, P. Foss and S. Liaaen-Jensen. 1985. *Synechococcus* spp. as likely zeaxanthin-dominant ultraphytoplankton in the North Atlantic. Limnol. Oceanogr., *30,* 412–414.

Harrison, W. G. 1980. Nutrient regeneration and primary production in the sea, *in* Primary productivity in the sea, P. G. Falkowski, ed., Plenum Press, NY, 433–460.

Haury, L. R., J. A. McGowan and P. H. Wiebe. 1978. Patterns and processes in the time-space scales of plankton distributions, *in* Spatial Patterns in Plankton Communities, J. H. Steele, ed., Plenum Press, NY, 277–327.

Haxo, F. T. 1985. Photosynthetic action spectrum of the coccolithophorid, *Emiliania huxleyi* (Haptophyceae): 19′ Hexanoyloxyfucoxanthin as antenna pigment. J. Phycol., *21,* 282–287.

Hooks, C. E., R. R. Bidigare, M. D. Keller and R. R. L. Guillard. 1988. Coccoid eukaryotic marine ultraphytoplankters with four different HPLC pigment signatures. J. Phycol., *24,* 571–580.

Hulburt, E. M. 1964. Succession and diversity in the plankton flora of the western North Atlantic. Bull. Mar. Sci. Gulf and Caribbean, *14,* 33–44.

—— 1966. The distribution of phytoplankton, and its relationship to hydrography, between Southern New England and Venezuela. J. Mar. Res., *24,* 67–81.

Hulburt, E. M., J. H. Ryther and R. R. L. Guillard. 1960. The phytoplankton of the Sargasso Sea off Bermuda. J. du Conseil, Conseil Permanent International pour l'Exploration de la Mer, *25,* 115–128.

Huntley, M. E., V. Marin and F. Escritor. 1987. Zooplankton grazers as transformers of ocean optics: A dynamic model. J. Mar. Res., *45,* 911–945.

Iturriaga, R. and J. Marra. 1988. Temporal and spatial variability of chroococcoid cyanobacteria, *Synechococcus* spp., specific growth rates and their contribution to primary production in the Sargasso Sea. Mar. Ecology Prog. Ser., *44,* 175–181.

Iturriaga, R. and B. G. Mitchell. 1986. Chroococcoid cyanobacteria: A significant component in the food web dynamics of the open ocean. Mar. Ecology Prog. Ser., *28,* 291–297.

Iturriaga, R. and D. A. Siegel. 1989. Microphotometric characterization of phytoplankton and detrital absorption in the Sargasso Sea. Limnol. Oceanogr., *34,* 1710–1730.

Jeffrey, S. W. 1974. Profiles of photosynthetic pigments in the ocean using thin-layer chromatography. Mar. Biol., *26,* 101–107.

—— 1976. A report of green algal pigments in the central North Pacific Ocean. Mar. Biol., *37,* 33–37.

Jenkins, W. J. 1982. On the climate of a subtropical ocean gyre: Decade timescale variations in water mass renewal in the Sargasso Sea. J. Mar. Res., *40*(Suppl.), 265–290.

—— 1988. Nitrate flux into the euphotic zone near Bermuda. Nature, *331,* 521–523.

Jenkins, W. J. and J. C. Goldman. 1985. Seasonal oxygen cycling and primary production in the Sargasso Sea. J. Mar. Res., *43,* 465–491.

Katz, E. J. 1969. Further study of a front in the Sargasso Sea. Tellus, *21,* 259–269.

Kawase, M. and J. L. Sarmiento. 1985. Nutrients in the Atlantic thermocline. J. Geophys. Res., *90,* 8961-8979.

Kiefer, D. A., R. J. Olson and O. Holm-Hansen. 1976. Another look at the nitrite and chlorophyll maxima in the central North Pacific. Deep-Sea Res., *23,* 1199–1208.

Kitchen, J. C., J. R. V. Zaneveld and H. Pak. 1982. Effect of particle size distribution and chlorophyll content on beam attenuation spectra. Appl. Optics, *21,* 3913–3918.

Klein, P. and B. Coste. 1984. Effects of wind-stress variability on nutrient transport into the mixed layer, Deep-Sea Res., *31,* 21–37.

Lai, D. Y. and P. L. Richardson. 1977. Distribution and movements of Gulf Stream rings. J. Phys. Oceanogr., *7,* 670–683.

Leetmaa, A. and A. D. Voorhis. 1978. Scales of motion in the subtropical convergence zone. J. Geophys. Res., *83,* 4589–4592.

Lewis, M. R., W. G. Harrison, N. S. Oakey, D. Herbert and T. Platt. 1986. Vertical nitrate fluxes in the oligotrophic ocean. Science, *234,* 870–873.

Lewis, M. R., N. Kuring and C. S. Yentsch. 1988. Global patterns of ocean transparency: Implications for the new production of the open ocean. J. Geophys. Res., *93,* 6847–6856.

Lorenzen, C. J. 1981. Chlorophyll *b* in the eastern North Pacific Ocean. Deep-Sea Res., *28,* 1049–1056.

McCartney, M. S. 1982. The subtropical recirculation of Mode waters. J. Mar. Res., *40*(Suppl.), 427–464.

Mandelli, E. F. 1972. The effect of growth illumination on the pigmentation of a marine dinoflagellate. J. Phycol., *8,* 367–369.

Marra, J., R. R. Bidigare and T. D. Dickey. 1990. Nutrients and mixing, chlorophyll and phytoplankton growth. Deep-Sea Res., *37,* 127–143.

Menzel, D. W. and J. H. Ryther. 1960. The annual cycle of primary production in the Sargasso Sea off Bermuda. Deep-Sea Res., *6,* 351–367.

—— 1961. Annual variations in primary production of the Sargasso Sea off Bermuda. Deep-Sea Res., *7,* 282–288.

Michaels, A. F., and M. W. Silver. 1988. Primary production, sinking fluxes and the microbial food web. Deep-Sea Res., *35,* 473–490.

Morel, A. 1988. Optical modeling of the upper ocean in relation to its biogenous matter content (Case I waters). J. Geophys. Res., *93,* 10,749–10,768.

Murphy, L. S. and E. M. Haugen. 1985. The distribution and abundance of phototrophic ultraplankton in the North Atlantic. Limnol. Oceanogr., *30,* 47–58.

Musgrave, D. L., J. Chou and W. J. Jenkins. 1988. Application of a model of upper-ocean physics for studying seasonal cycles of oxygen. J. Geophys. Res., *93,* 15,679–15,700.

Pak, H., D. A. Kiefer and J. C. Kitchen. 1988. Meridional variations in the concentration of chlorophyll and microparticles in the North Pacific Ocean. Deep-Sea Res., *35,* 1151–1171.

Parsons, T. R., M. Takahashi and B. Hargrave. 1984. Biological Oceanographic Processes, 3rd edition, Pergamon Oxford, U.K., 330 pp.

Platt, T., D. V. Subba-Rao and B. Irwin. 1983. Photosynthesis of picoplankton in the oligotrophic ocean. Nature, *301,* 702–704.

Riley, G. A., 1957. Phytoplankton of the north central Sargasso Sea. Limnol. Oceanogr., *2,* 252–270.

Riley, G. A., H. Stommel and D. F. Bumpus. 1949. Quantitative ecology of the plankton of the western North Atlantic. Bull. Bingham Oceanogr. Coll., *12,* 1–169.

Roman, M. R. C. S. Yentsch, A. L. Gauzens and D. A. Phinney. 1986. Grazer control of the fine-scale distribution of phytoplankton in warm-core Gulf Stream rings. J. Mar. Res., *44,* 795–813.

Ryther, J. H. and D. W. Menzel. 1960. The seasonal and geographic range of primary production in the western Sargasso Sea. Deep-Sea Res., *6,* 235–238.

Sampson, R. J. 1978. Surface-II Graphics System, Kansas Geological Survey, Lawrence, Kansas, 240 pp.

Schmitt, R. W., P. S. Bogden and C. E. Dorman. 1989. Evaporation minus precipitation and density fluxes for the North Atlantic. J. Phys. Oceanogr., *19,* 1208–1221.

Schroeder, E., H. Stommel, D. Menzel and W. Sutcliffe, Jr. 1959. Climatic stability of eighteen degree water at Bermuda. J. Geophys. Res., *64,* 363–366.

Siegel, D. A. and T. D. Dickey. 1987a. Observations of the vertical structure of the diffuse attenuation coefficient spectrum. Deep-Sea Res., *34,* 547–563.

—— 1987b. On the parameterization of irradiance for open ocean photoprocesses. J. Geophys. Res., *92,* 14,648–14,662.

Simonot, J.-Y. and H. LeTreut. 1986. A climatological field of mean optical properties of the world ocean. J. Geophys. Res., *91*, 6642–6646.

Smetacek, V. S. 1985. Role of sinking diatom life-history cycles: Ecological, evolutionary and geological significance. Mar. Biol., *84*, 239–251.

Smith, R. C. and K. S. Baker. 1978a. The bio-optical state of ocean waters and remote sensing. Limnol. Oceanogr., *23*, 247–259.

—— 1978b. Optical classification of natural waters. Limnol. Oceanogr., *23*, 260–267.

—— 1981. Optical properties of the clearest natural waters. Appl. Optics, *20*, 177–184.

—— 1984. The analysis of ocean optical data. Proc. Soc. Photo-Optical Instr. Eng., *489*, Ocean Optics VII, 119–126.

—— 1985. Spatial and temporal patterns in pigment biomass in Gulf Stream Warm-Core Ring 82B and its environs. J. Geophys. Res., *90*, 8859–8870.

Smith, R. C., K. S. Baker and P. Dustan. 1981. Fluorometric techniques for the measurement of oceanic chlorophyll in the support of remote sensing, Scripps Institution of Oceanography Technical Report, *81–17*, 14 pp.

Smith, R. C., R. R. Bidigare, B. B. Prézelin, K. S. Baker and J. M. Brooks. 1987a. Optical characterization of primary production across a coastal front. Mar. Biol., *96*, 575–591.

Smith, R. C., C. R. Booth and J. L. Star. 1984. Oceanographic biooptical profiling system. Appl. Optics, *23*, 2791–2797.

Smith, R. C., O. B. Brown, F. K. Hoge, K. S. Baker, R. H. Evans, R. N. Swift and W. E. Esaias. 1987b. Multiplatform sampling (ship, aircraft, and satellite) of a Gulf Stream warm core ring. Appl. Optics, *26*, 2068–2081.

Smith, R. C., J. Marra, M. J. Perry, K. S. Baker, E. Swift, E Buskey and D. A. Kiefer. 1989. Estimation of a photon budget for the upper ocean in the Sargasso Sea. Limnol. Oceanogr., *34*, 1677–1697.

SooHoo, J. B., D. A. Kiefer, D. J. Collins and I. S. McDermid. 1986. In vivo fluorescence excitation and absorption spectra of marine phytoplankton: I. Taxonomic characteristics and responses to photoadaptation. J. Plank. Res., *8*, 197–214.

Spitzer, W. S. and W. J. Jenkins. 1989. Rates of vertical mixing, gas exchange and new production: Estimates from seasonal gas cycles in the upper ocean near Bermuda. J. Mar. Res., *47*, 169–196.

Talley, L. D. and M. E. Raymer. 1982. Eighteen degree water variability. J. Mar. Res., *40*(Suppl.), 757–775.

Tyler, J. 1966. Report on the second meeting of the joint group of experts on photosynthetic radiant energy, UNESCO Technical Paper, *2*, 11 pp.

Voorhis, A. D. 1969. The horizontal extent and persistence of thermal fronts in the Sargasso Sea. Deep-Sea Res., *16*, 331–337.

Voorhis, A. D. and J. G. Bruce. 1982. Small-scale stirring and frontogenesis in the subtropical convergence of the western North Atlantic. J. Mar. Res., *40*(Suppl.), 801–821.

Warren, B. A. 1972. Insensitivity of subtropical mode water characteristics to meterological fluctuations. Deep-Sea Res., *19*, 1–19.

Worthington, L. V. 1959. The 18° water in the Sargasso Sea. Deep-Sea Res., *5*, 297–305.

—— 1976. On the North Atlantic circulation. The Johns Hopkins Oceanographic Studies, *6*, 110 pp.

Received: *2 November, 1989;* revised: *12 February, 1990.*